Precambrian Research, 52 (1991) 71–96
Elsevier Science Publishers B.V., Amsterdam

Archaean orogenic ultrapotassic magmatism: an example from the southern Abitibi greenstone belt

M.R. Laflèche [a], C. Dupuy [a] and J. Dostal [b]

[a] *C.N.R.S., Centre Géologique et Géophysique, Université de Montpellier II, Place Eugène Bataillon, 34095 Montpellier Cedex 5, France*

[b] *Department of Geology, Saint Mary's University, Halifax, N.S. B3H 3C3, Canada*

(Received June 26, 1990; revised and accepted January 28, 1991)

ABSTRACT

Laflèche, M.R., Dupuy, C. and Dostal, J., 1991. Archaean orogenic ultrapotassic magmatism: an example from the southern Abitibi greenstone belt. Precambrian Res., 52: 71–96.

The Cléricy Pluton in the southern Abitibi greenstone belt of Québec is a syenitic intrusion cross-cut by nordmarkitic dykes. It is probably one of the oldest known ultrapotassic intrusions (about 2.7 Ga). It crystallized in a crustal environment under low P_{H_2O} (<2.5 kbar) and low f_{O_2} conditions. Most trace elements behaved as compatible elements suggesting that sphene and apatite were involved together with clinopyroxene during low-pressure crystal fractionation. The large range of initial isotopic ratios (calculated for 2.68 Ga, ϵ_{Nd} -1.9 to $+2.3$), as well as the trace element distribution, suggest that the syenitic pluton is the product of differentiation from a parental magma with a composition similar to that of Timiskaming-type Archaean shoshonites contaminated by a crustal component. On the other hand, the nordmarkitic dykes are probably the result of crustal anatexis of metasedimentary rocks and some addition of the syenitic magma. The Cléricy peralkaline syenite differs chemically from typical intraplate syenites in being saturated with respect to quartz, and displaying lower Ti and HFSE contents. It is related to an ultrapotassic volcano-plutonic event, which characterized the last 20 Ma of igneous activity in the Abitibi greenstone belt. It may represent an increased rate of convergence of small heterogeneous plates during a subduction-driven accretion tectonic event which possibly marked the culmination of the Kenoran Orogeny in the Superior Province of the Canadian Shield.

Introduction

Most modern petrological and geochemical studies of syenitic intrusions involve rocks of Phanerozoic age. There are relatively few studies of Proterozoic syenites (e.g. Badham, 1979; Upton and Emeleus, 1987; Santosh et al., 1989) and it seems that there are no detailed studies of Archaean syenites. Although volumetrically insignificant compared to sub-alkaline rocks, ancient syenites are important in several respects. They may provide information on the nature of the underlying mantle as well as on the petrological processes involved during the formation of Archaean ultrapotassic magmas.

The purpose of this paper is to present a detailed geochemical and petrological study of the Cléricy Pluton, one of the oldest known Archaean ultrapotassic syenitic intrusions. This intrusion, with ultrapotassic volcanic rocks of the southern Abitibi belt shares certain geochemical features with modern shoshonitic rocks. The occurrence of this type of magmatism in tectono-stratigraphic environments of late Archaean greenstone belts of North America (2.7 Ga), may suggest a primitive type of plate tectonics (e.g. Brooks et al., 1982; Wyman and Kerrich, 1989).

0301-9268/91/$03.50

Geological setting

The east–west trending Abitibi greenstone belt is about 800 km long and 240 km wide and is the largest plutono-metavolcanic belt of the Superior Province (e.g. Card, 1990) and of the Canadian Shield (Goodwin and Ridler, 1970). It is bounded to the north by the Archaean Quetico gneissic–plutonic Subprovince, to the west by the Kapuskasing structural zone (Percival, 1986), and to the south and east by the Archaean Pontiac Subprovince and the Proterozoic Grenville Province.

The southern part of the Abitibi belt is composed of low- to intermediate-grade metamorphosed volcanic (e.g. Gélinas et al., 1977), sedimentary and plutonic rocks (e.g. Rive et al., 1990) intruded by early and middle Proterozoic dyke swarms (e.g. Fahrig, 1985) (Fig. 1). The southern Abitibi belt is bounded to the south by the Larder Lake–Cadillac Break (shear-zone) separating the greenstone belt from Archaean metasedimentary and gneisso-plutonic rocks of the Pontiac Subprovince (Goulet, 1978; Dimroth et al., 1983).

In Québec, the supracrustal rocks of the southern Abitibi belt, can be subdivided into five volcanic groups which locally overlap (OGS-MERQ, 1984; Jensen, 1985).

(1) The bimodal calc-alkaline assemblages of the Hunter Mine Group (Laflèche and Ludden, 1990) are the oldest volcanic rocks of the southern Abitibi belt (2730 to 2713 Ma, Mortensen, 1987; Corfu et al., 1989).

(2) In eastern Ontario and Québec, the komatiitic and tholeiitic volcanic rocks of the Stroughton–Roquemaure and Malartic Groups overly the Hunter Mine Group. Flow-banded rhyolites at the base of the Stroughton–Roquemaure Group are 2714±2 Ma old (Corfu et al., 1989).

(3) The Kinojévis Group overlies the two previous groups (Jensen, 1985) and is characterized by a monotonous series of tholeiitic basalts (Dimroth et al., 1985) and rare komatiitic flows. It is intruded, in its lower part, by numerous sub-volcanic gabbroic dykes and sills.

(4) The Blake River Group (2703–2698 Ma, Mortensen, 1987; Corfu et al., 1989) is located between the Cadillac–Larder Lake Break to the south and the Porcupine–Destor Break to the north (Ambrose, 1941). Regional metamorphism ranges from sub-greenschist in the

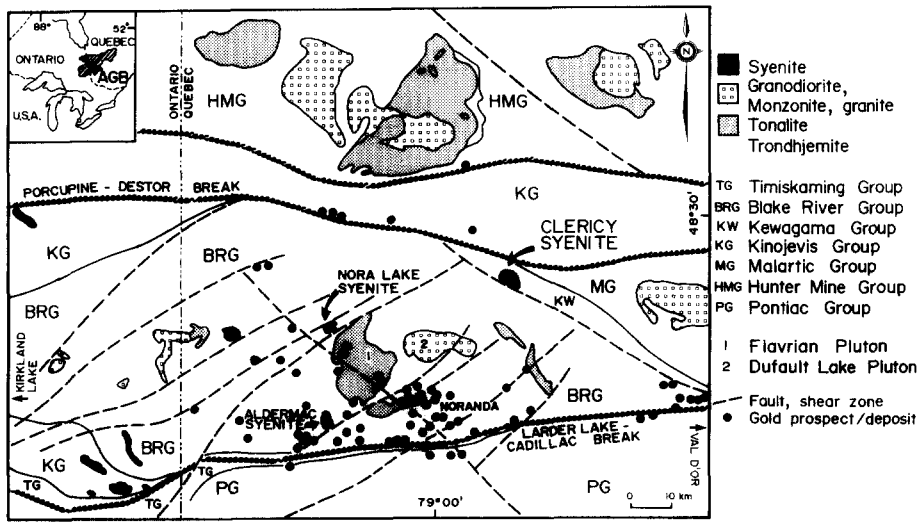

Fig. 1. Simplified geological map of the southern Abitibi belt in northwest Ontario and northeast Québec (modified from OGS-MERQ, 1984; Rive, 1989).

north to lower greenschist facies in the south (Jolly, 1978; Dimroth et al., 1983). Bimodal volcanic rocks of the Blake River Group (Gélinas et al., 1984; Ujike and Goodwin, 1987) are intruded by a paraconcordant metamorphosed trondhjemite–tonalite suite and by younger discordant unmetamorphosed granodioritic (Rive et al., 1990) and ultrapotassic intrusions including the Cléricy, Aldermac and Nora Lake plutons (Fig. 1)

(5) The Timiskaming volcano-sedimentary Group (Cooke and Moorhouse, 1969) unconformably overlies the Kinojevis and Blake River Groups in northeastern Ontario and northwestern Québec (Jensen, 1985). The Timiskaming is dated at 2.700±0.1 Ga (Basu et al., 1984) and it contains numerous shoshonitic and trachytic massive flows and pyroclastic rocks (Ujike, 1985) associated with alluvial–fluvial sediments (Ojakangas, 1985). Both volcanic and sedimentary rocks are intruded by numerous syenitic dykes, sills and plugs (e.g. Kerrich and Watson, 1984). The youngest syenitic pluton of the Timiskaming Group gives an age of 2680±1 Ma (Corfu et al., 1989) which is similar to the age of late- to post-kinematic granodiorite and monzogranite intrusions of the Abitibi belt (e.g. Gariépy and Allègre, 1985; Corfu et al., 1989).

The effects of pre-Kenoran events were largely obliterated by the pervasive polyphase deformation, regional metamorphism and wide-spread plutonism of the last major orogenic event, the Kenoran Orogeny, at 2.73–2.65 Ga (Card, 1990). The polyphase tectonism involved early ductile deformation under north–south subhorizontal regional compression (e.g. Dimroth et al., 1983) and low-pressure metamorphism (e.g. Jolly, 1980), followed by brittle deformation, still under north–south compression and dextral transcurrent faulting and shearing (e.g. Robert, 1989).

The Cléricy ultrapotassic intrusion

The Cléricy ultrapotassic intrusion is an oval-shaped stock, 3.5 km by 1.5 km, located approximately 1.5 km south of the Porcupine–Destor Break between the metavolcanic rocks of the Blake River Group and the metasedimentary rocks of the Kewagama Group (Fig. 2). It cross-cuts a strongly magnetized pyroxenitic body, 0.3 km wide and 2.5 km long. The Cléricy intrusion is composed of two syenitic components: a mafic clinopyroxene-rich (ca. 35%) and a feldspar-rich one (ca. 50%). Both components are intruded by nordmarkitic dykes, 0.1–225 m wide (which form 10 to 15% of the pluton). These fined-grained dykes are massive and homogeneous and usually cross-cut the igneous layering.

Igneous layering involving clinopyroxene cumulates forming numerous schlieren (or enclaves) and mineral-graded layering on various scales (cm to 1.5 m), is visible in the mafic syenite. Turbulent magmatic flow is suggested by the presence of channels and oblique laminations. In addition, the presence of softly deformed layers of clinopyroxene cumulates forming contorted laminae in the feldspar-rich syenite may suggest magmatic mixing between the clinopyroxene cumulates and the felsic component.

The Cléricy Pluton has undergone brittle fractionation and faulting during, at least, two late- or post-orogenic strain increments. The first one is characterized by subvertical, east–

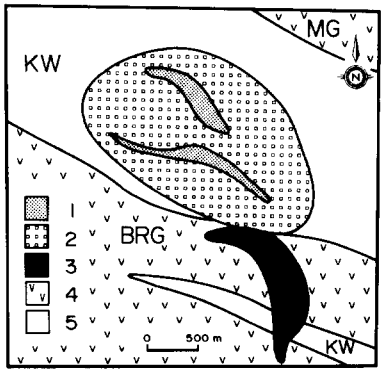

Fig. 2. Simplified geological map of the Cléricy intrusion. The contact with the pyroxenitic body is extrapolated from geophysical and drill-hole data. *1*=nordmarkite; *2*=syenite; *3*=pyroxenite; *4*=metavolcanic rocks; *5*=metasedimentary rocks.

west striking faults with a strike-slip dextral throw of less than 0.5 m and the second one by late subvertical north–south striking faults with a dextral throw of less than 2.0 m. The second event is probably Proterozoic in age since it also affects the lower Proterozoic Huronian Cobalt sedimentary rocks (Camiré et al., in prep).

Petrography

According to the modal classification of Streckeisen (1976), the composition of the Cléricy intrusion ranges from alkali-feldspar syenite to alkali-feldspar quartz syenite and alkali-feldspar granite. In the present study, the nordmarkites (Sorensen, 1974) represent the late alkali-feldspar bearing granitic dykes.

Mafic and felsic syenites

The mafic and felsic syenites are distinguished by their relative proportions of alkali feldspar and clinopyroxene (mafic syenites, 20–50% clinopyroxene; felsic syenites, 5–10% clinopyroxene; clinopyroxene cumulates, 90–95% clinopyroxene). Interstitial quartz occurs locally in the felsic syenites. The pluton is also characterized by the absence of olivine (or olivine pseudomorphs), orthopyroxene, plagioclase, igneous amphibole, biotite and the scarcity of Fe–Ti oxides.

In the Cléricy intrusion, zoned perthitic alkali-feldspar phenocrysts, 5 to 9 mm in size, are commonly subhedral and locally surrounded by a thin layer of albite. Unzoned alkali feldspar forming the fine-grained matrix is also subhedral. Clinopyroxene phenocrysts (1.5 to 5 mm in size), partly replaced by stilpnomelane, are subhedral, zoned and twinned (less than 5%), whereas matrix clinopyroxenes (<0.5 mm in size) are anhedral and rarely zoned. Identified accessory minerals include sphene, calcite, apatite, pyrrhotite and non-titaniferous iron oxides. Sphene, apatite and rare calcite are observed as inclusions in some clinopyroxene.

Microdeformation, shown by undulatory extinction of quartz and kinked stilpnomelane also suggests that the post-metamorphic Cléricy intrusion was affected by late orogenic strain increments.

Nordmarkitic dykes

Nordmarkitic dykes differ from the syenites in containing more abundant quartz (>5%) and minor clinopyroxene (<5%). Two mineral assemblages are present: a primary magmatic assemblage composed of perthitic alkali feldspar, quartz, clinopyroxene, sphene and apatite, and a secondary one, resulting from hydrothermal alteration, characterized by the presence of riebeckite, winchite, actinolite, stilpnomelane, and thin layers of albite surrounding alkali-feldspar phenocryst.

Mineral chemistry

Clinopyroxene

Clinopyroxene compositions (Table 1) display a large variation in all facies of the Cléricy intrusion (Figs. 3 and 4). According to the classification of Morimoto et al. (1988), they are Ca–Na pyroxenes (augite–aegirine). On the Mg–(Fe^{2+} + Mn)–Na ternary diagram of Larsen (1976) (Fig. 3), the chemical evolution of aegirine–augite towards Na-rich compositions is characteristic of strongly undersaturated alkaline magmatic suites. An evolutionary trend similar to that of the Cléricy Pluton has been observed in the Sande Cauldron syenitic and nordmarkitic complex of the Oslo rift area (Andersen, 1984). Low Al and Ti contents of the clinopyroxene reflect respectively magmatic differentiation at low pressure (Wass, 1979) and low Ti content of the parental magma.

Magmatic differentiation from mafic to felsic syenite is shown in Fig. 4 by an increase in Fe and Na in the clinopyroxene phenocrysts. Fe and Na enrichment is also observed in the microphenocrysts, reflecting contemporary crystallization from an interstitial differen-

TABLE 1
Representative microprobe analyses of clinopyroxenes

	Cpx cumulate 6155 cpx 1			6153 cpx 31		Felsic syenite 6156 cpx 40		cpx 44		Nordmarkite 6157 cpx 10		cpx 13	
	core	mantle	rim	core	rim	core	rim	core	rim	core	rim	core	rim
SiO_2	53.70	53.25	52.83	52.42	52.24	52.38	53.35	52.73	52.47	53.54	53.74	53.56	53.08
TiO_2	0.35	0.32	0.36	0.40	0.35	0.37	0	0.11	0	0.07	0.35	0.05	0.04
Al_2O_3	1.00	1.18	1.07	1.52	0.86	1.35	0.82	0.71	1.11	0.40	0.39	0.51	0.39
FeO	12.47	14.12	16.41	12.12	7.90	13.05	17.49	14.45	16.53	17.60	16.93	15.82	17.75
MnO	0.43	0.34	0.33	0.34	0.18	0.38	0.47	0.47	0.41	0.55	0.52	0.45	0.46
MgO	10.12	9.45	8.15	10.79	14.00	9.82	6.34	7.82	7.51	7.60	7.60	7.75	6.99
CaO	18.77	17.89	16.99	19.31	21.05	18.16	12.08	16.95	15.31	14.13	11.94	15.21	14.17
Na_2O	3.47	3.88	4.24	3.37	2.45	3.68	6.78	4.52	5.25	5.90	7.19	4.84	5.89
Total (wt.%)	100.31	100.43	100.38	100.27	99.03	100.20	99.00	97.74	99.40	99.79	98.66	98.19	98.77
Cations per 8 oxygens													
Si	1.991	1.977	1.976	1.937	1.921	1.963	2.034	2.014	1.990	2.002	2.006	2.040	2.006
Al(IV)	0.009	0.023	0.024	0.063	0.037	0.037	0	0	0	0	0	0	0.000
Al(VI)	0.035	0.028	0.023	0.003	0	0.023	0.037	0.032	0.049	0.018	0.017	0.023	0.017
Fe^{2+}	0.183	0.182	0.225	0.096	0	0.149	0.163	0.194	0.186	0.148	0.058	0.251	0.162
Fe^{3+}	0.203	0.257	0.288	0.279	0.244	0.260	0.395	0.268	0.334	0.400	0.471	0.253	0.400
Mg	0.559	0.523	0.454	0.594	0.769	0.549	0.360	0.445	0.420	0.422	0.423	0.440	0.394
Mn	0.014	0.011	0.011	0.011	0.006	0.012	0.015	0.015	0.013	0.017	0.016	0.014	0.015
Ti	0.010	0.009	0.010	0.011	0.010	0.010	0	0.003	0	0.002	0.010	0.001	0.001
Ca	0.746	0.712	0.681	0.765	0.832	0.729	0.494	0.694	0.616	0.564	0.478	0.621	0.574
Na	0.250	0.279	0.308	0.241	0.175	0.267	0.501	0.335	0.382	0.426	0.521	0.357	0.432

FeO as total iron.
Mineral analyses were obtained with an automated spectrometer DATAMIN CAMEBAX electron microprobe using a 20-kV acceleration voltage. The analytical current was 20 nA.

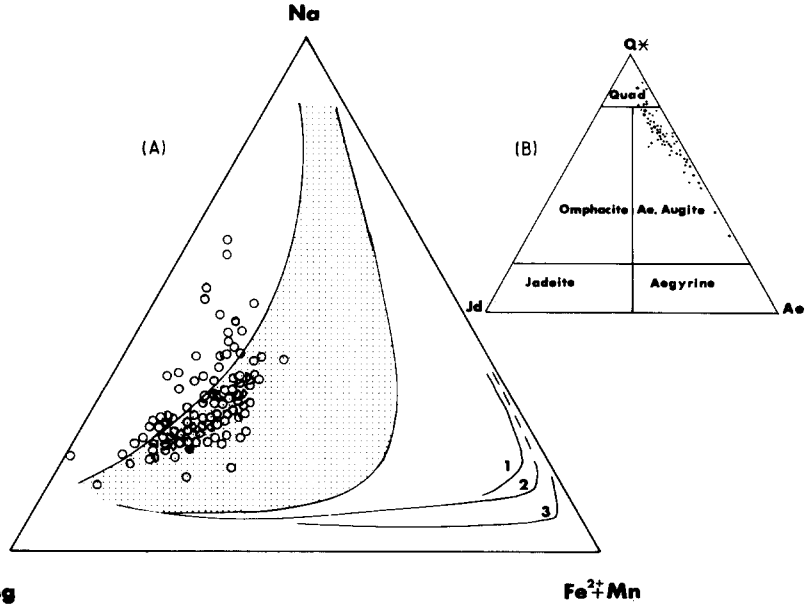

Fig. 3. A. Major element variations for pyroxenes (open circles). Compositions are plotted in terms of atomic percent of the element shown. Shaded area identifies the field of strongly under-saturated alkaline magmatic suites and lines *1* to *3* represent examples of SiO_2 oversaturated peralkaline magmatic suites (after Larsen, 1976). B. Classification of "non-quadrilateral" pyroxenes according to Morimoto et al. (1988).

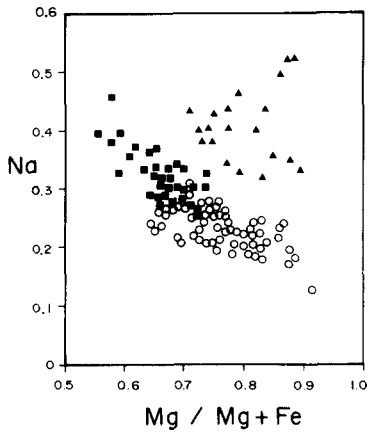

Fig. 4. Na vs. (Mg/Mg+Fe) variations for selected pyroxenes of the Cléricy Pluton. Open circle, clinopyroxene cumulate; square, felsic syenite; triangle, nordmarkite. Element in atomic percent from structural formula.

tiated magma. The clinopyroxenes of the nordmarkites do not plot on this differentiation trend. They are enriched in Na and their high Mg/Mg+Fe ratios do not reflect the differentiated nature of the nordmarkitic magmas (e.g. Fig. 4 and Table 1: clinopyroxene 11 and 13). According to Deer et al. (1978) and Luhr and Carmichael (1980), this can be explained by $NaFe^{3+}$ substitution for $Ca(MgFe^{2+})$ which is favoured by an increase in f_{O_2}.

Clinopyroxenes in the mafic syenites display inverse or normal zonation (e.g. clinopyroxenes 1 and 31, Table 1). The zoning is marked by a variation of the Mg/Mg+Fe ratio which cannot be simply explained by equilibrium or fractional crystallization; it is interpreted as evidence for magmatic mixing processes (e.g. Sakuyama, 1978).

Feldspars

The Cléricy intrusion is an hypersolvus syenite characterized by the presence of one type of zoned alkali feldspar. This suggests a rapid cooling and shallow depth ($P_{H_2O} \leqslant 2.5$ kbar, Martin and Bonin, 1976) crystallization of the magma chamber. Perthitic feldspar phenocrysts are sodic (Ab_{99}) and potassic (Or_{99}) and reflect sub-solvus reequilibration. Only one analysis has an intermediate composition of $Ab_{41}Or_{59}$. However, complex chemical zonation is shown by macroscopic and microscopic textures. In the nordmarkites, perthitic alkali-feldspar phenocrysts are commonly surrounded by a thin layer of secondary albite. Sharp contacts between albitic perthite and secondary albite suggest that the appearance of the latter postdates the sub-solidus perthitisation of the alkali feldspar. Secondary albite appears to be a product of pneumatolitic alteration (Martin, 1969).

Amphiboles

In the nordmarkitic dykes, fine acicular amphiboles have the composition of magnesian riebeckite and winchite. Rare fibrous crystals of Ca-rich actinolite are also observed surrounding clinopyroxene phenocrysts in clinopyroxene cumulates. According to Allen and Boettcher (1978), low-pressure crystallization of amphibole can be qualitatively inferred from the low abundance of AlVI in the octahedral site of magnesian riebeckite, winchite and actinolite. Furthermore, the stability field of actinolite limits the temperature and pressure to those usually observed in greenschist facies.

Geochemistry

Analytical techniques

135 samples were analysed for major elements. From these, 28 representative samples crushed in an agate mortar were analysed for major, rare earth (REE) and trace elements. Zr, Y, Nb and Ba were determined by X-ray fluorescence at the St. Mary University of Halifax (Canada). Li, Rb, Sr, V, Cr, Co, Ni, Cu and Zn were determined using an atomic absorption technique at the "Laboratoire de Géochimie des Eléments Traces du C.G.G." of the C.N.R.S. at Montpellier (France) where REE, Sc, Hf, Th and Ta were also analysed by I.N.A. Further details on analytical procedures and precision are given in Dostal et al. (1986). Five whole-rock samples and one clinopyrox-

ene concentrate were selected for the isotopic determinations. The clinopyroxenes (2–3 mm in size) were hand-picked under a binocular microscope, washed in a ultrasonic bath and rinsed with cold HCl-2N. The separation of Sr and Nd was performed using a standard ion exchange chromatography technique according to the procedure of Mahnes et al. (1978) and Richard et al. (1976). Chemical and loading blanks are considered negligible (<2 ng). Sr and Nd isotopic ratios are normalized to $^{86}Sr/^{88}Sr=0.1194$ and $^{144}Nd/^{146}Nd=0.7219$, respectively. Values for LaJolla standard yield $^{143}Nd/^{144}Nd=0.51186\pm3$ (2σ) and NBS987 are $^{87}Sr/^{86}Sr=0.71025\pm4$ (2σ). Error on $^{87}Sr/^{86}Sr$ and $^{143}Nd/^{144}Nd$ are quoted in Table 3 at 95% confidence level, and are based on within-run statistics. Sm and Nd were determined by isotopic dilution with a precision of 0.3% on the $^{147}Nd/^{144}Nd$ ratio. Rb and Sr data reported in Table 3 are an average of triplicate analyses obtained by atomic absorbtion spectroscopy with a precision better than 5% excepted for Rb in the clinopyroxene concentrate (50%).

Major and trace element data

Major elements

Compared to intraplate syenites, which are commonly under-saturated (McBirney and Aoki, 1968; Currie et al., 1986; Bardintzeff et al., 1988), and rarely peralkaline (Baker, 1975; Wagner et al., 1988), the syenites of the Clér-icy intrusion are peralkaline and saturated with respect to quartz. In this regard, they are similar to orogenic potassic magmatic suites (Foley et al., 1987) but enriched in Na_2O and K_2O. This is corroborated by the presence of acmite in the C.I.P.W. norm (Table 2), lack of plagioclase and abundance of Na-rich clinopyroxene. Given that the mineral assemblages found in K-rich igneous rocks are highly dependent on bulk composition (e.g. Wendlandt and Eggler, 1980; Yoder, 1986), the suppression of Ca-plagioclase crystallization in the Clér-icy Pluton, reflects the particular composition of the studied perlkaline syenites which are marked by very low CaO/Al_2O_3 ratio (<0.25) and high K_2O/Al_2O_3 ratio (>0.32).

Major elements display a large variation reflecting the different petrographic characteristics of each intrusive facies. SiO_2 content varies from 49 to 76 wt.%; it is less than 54% in clinopyroxene-cumulates, 56–58% in mafic syenites, 60–67% in felsic syenites, and more than 68% in nordmarkites. FeO, MgO, CaO, MnO, TiO_2, and P_2O_5 abundances (Fig. 5) decrease with increasing differentiation, whereas Al_2O_3, Na_2O and K_2O increase along with the silica content up to 65 wt.% SiO_2 and then decrease. The large dispersion of K_2O, in samples which have 55–65 wt.% SiO_2, reflects the heterogeneity of the alkali feldspar distribution. The mafic syenites display a large variation in composition due to the relative proportions of the mafic and feldspathic components. They are distinguished from the felsic syenites by higher abundances of CaO, FeO, MgO, P_2O_5 and TiO_2, and lower SiO_2, Al_2O_3, K_2O and Na_2O. Compared to the mafic and felsic syenites, the nordmarkites have higher SiO_2 and Na_2O contents and 4.4–5 wt.% K_2O.

Alkali and alkali-earth elements

The extensive variations in the concentrations of alkali and alkaline-earth elements (Sr, Rb, Ba) can be related to the ultrapotassic and shoshonitic nature of the parental magma and to the relative abundance of K-feldspar in the various intrusive facies. The decrease of Sr (3750–100 ppm) and Ba (10,000–600 ppm) contents with increasing SiO_2, as well as the variation of the Rb/Sr ratio (0.015 in mafic syenites and up to 0.50 in felsic syenites) may suggest the involvement of K-feldspar crystallization in the differentiation process. In addition, the concentrations of alkali elements were probably slightly modified by the alteration processes indicated by secondary minerals such as stilpnomelane, calcite, riebeckite and actinolite. For example, K/Rb is higher in

TABLE 2

Major and trace element composition of selected samples of the Cléricy ultrapotassic intrusion

	Cpx cumulate			Mafic syenite							
	6155	C6155	6169	751	816	832	915	6175	566	782	812
SiO_2	53.90	53.90	47.10	57.40	57.70	57.20	56.00	56.10	59.70	62.90	63.50
TiO_2	0.40	0.46	1.26	0.45	0.61	0.32	0.72	0.51	0.28	0.55	0.48
Al_2O_3	4.55	0.56	4.50	12.46	10.00	11.56	7.16	13.26	13.69	15.70	15.10
Fe_2O_3	11.83	14.30	11.08	5.45	6.50	5.68	7.97	3.95	4.30	2.83	3.48
MnO	0.27	0.30	0.24	0.11	0.14	0.11	0.19	0.11	0.09	0.07	0.05
MgO	8.78	9.17	10.95	4.12	4.55	4.60	5.95	4.78	2.58	1.13	0.94
CaO	13.73	17.80	14.65	7.36	10.01	8.96	13.11	9.55	6.17	2.77	2.70
Na_2O	3.62	3.45	2.10	2.32	2.53	2.12	2.65	4.42	4.00	4.70	4.42
K_2O	1.90	0	2.57	8.23	6.32	7.40	4.00	1.84	7.40	7.90	8.48
P_2O_5	0.67	0	1.27	0.68	0.98	1.02	1.39	0.19	0.39	0.23	0.15
H_2O^-	0.02	0	2.02	0.19	0.02	0.03	0.17	0.23	0.14	0.21	0.21
CO_2	0.29	n.a.	n.a.	0.58	0.20	0.60	0.45	0.45	0.18	0.34	0.32
Total (wt%)	99.96	99.94	97.74	99.35	99.56	99.60	99.76	95.39	98.92	99.33	99.83
CIPW Norm											
Q	0	5.64	0	0	0.57	0	2.43	2.57	0	0.77	3.06
Or	11.38	0	12.47	40.38	36.24	41.44	22.79	11.44	33.53	46.72	49.85
Lc	0	0	2.81	7.68	0	2.00	0	0	9.60	0	0
Kp	0	0	0	0	0	0	0	0	0	0	0
Ab	12.99	2.72	0	14.21	15.76	16.874	14.02	39.36	24.80	36.78	30.28
Ne	0	0	5.06	2.50	0.00	0.65	0	0	3.13	0	0
Al	0	0	0	0	0	0.16	0	11.43	0	0	0
Co	0	0	0	0	0	0	0	0	0	0	0
Ac	9.00	10.16	8.33	1.25	4.43	0	5.77	0	3.38	2.13	2.60
Di-Ca	27.13	34.86	28.77	14.00	17.78	16.07	22.87	15.53	12.21	5.17	5.19
Di-Mg	23.28	29.93	24.70	11.95	15.20	13.74	19.60	13.27	6.71	4.33	4.33
Di-Fe	0.14	0.16	0.13	0.15	0.16	0.15	0.16	0.15	5.03	0.18	0.19
Wo	0	0	0	0	0	0	0	0	0.16	0	0
En	0	0	0	0	0	0	0	0	0	0	0
Fs	13.64	15.71	0	0	6.50	0	8.11	3.17	0.00	2.38	3.27
Fo	0	0	2.84	0	0	0	0	0	0	0	0
Fa	0.19	0	9.20	3.96	0	3.94	0	0	0	0	0
Ab	1.48	0	2.93	1.53	2.08	2.24	2.93	0.44	0.89	0.50	0.33
Il	0.77	0.83	2.53	0.88	1.13	0.61	1.32	1.02	0.56	1.05	0.91
Ml	0	0	0.23	1.49	0.16	2.15	0	1.57	0	0	0
Hm	0	0	0	0	0	0	0	0	0	0	0
Ru	0	0	0	0	0	0	0	0	0	0	0
Sp	0	0	0	0	0	0	0	0	0	0	0
Σ	100	100	100	100	100	100	100	100	100	100	100
Li	16	n.a.	77	9	9	8	10	27	12	5	4
Rb	40	n.a.	165	151	120	141	83	56	169	149	172
Sr	1715	n.a.	2230	2125	2895	2450	3000	407	1435	1375	2550
Ba	1002	n.a.	1680	8569	9824	10 555	7080	525	5674	3892	5116
Sc	21.1	19.9	25.1	11.2	13.7	12.6	18.1	9.2	6.4	3.4	4.6
V	200	253	171	89	111	88	140	78	80	56	56
Cr	320	303	385	92	120	102	157	109	95	29	34
Co	28.7	25.4	50.7	15.2	18.4	16.6	24.2	14.7	9.7	5.0	6.4

Felsic syenite						Nordmarkite					
842	874	894	897	930	961	795	799	866	899	927	6178
63.00	62.70	62.30	67.30	62.90	59.70	72.00	68.10	71.90	71.70	75.60	69.80
0.48	0.50	0.11	0.16	0.39	0.58	0.14	0.24	0.08	0.12	0.08	0.13
16.47	15.53	15.32	15.55	14.80	14.45	14.39	15.22	14.24	14.90	11.94	16.49
2.90	3.21	3.63	1.74	3.24	3.77	0.84	1.25	0.93	0.94	0.33	0.90
0.07	0.05	0.07	0.02	0.06	0.10	0.01	0.03	0.01	0.01	0.01	0.02
0.97	1.17	1.52	0.54	1.20	1.35	0.19	1.29	0.41	0.27	0.22	0.28
2.39	3.34	3.65	1.35	3.70	4.65	0.40	1.10	0.45	0.20	0.28	0.80
4.62	3.34	4.00	4.39	3.74	4.33	6.02	5.85	5.64	6.43	5.93	6.00
7.98	9.60	8.16	7.94	8.20	7.68	4.68	4.95	5.05	4.43	4.60	4.87
0.21	0.37	0.30	0.14	0.23	0.98	0.08	0.10	0.08	0.05	0.11	0.08
0.02	0.06	0.06	0.01	0.12	0.09	0.06	0.06	0.05	0.05	0.09	0.16
0.64	0.32	0.26	0.39	0.36	0.42	0.28	0.28	0.35	0.18	0.15	0.21
99.75	100.19	99.38	99.53	98.94	98.10	99.09	98.47	99.19	99.28	99.84	99.74
0.73	0.79	0.47	8.81	3.30	0	20.14	11.85	20.04	17.88	32.85	13.60
47.23	57.01	47.90	47.10	49.37	45.62	28.11	29.85	30.30	26.51	27.77	27.94
0	0	0	0	0	1.03	0	0	0	0	0	0
0	0	0	0	0	0	0	0	0	0	0	0
39.15	26.54	33.13	35.90	31.03	32.01	48.73	50.52	45.81	52.61	36.56	49.28
0	0	0	0	0	0.33	0	0	0	0	0	0
0.62	0	0	0	0	0	0	0.66	0	0	0	3.40
0	0	0	0	0	0	0	0	0	0	0	0.06
0	1.64	0.43	1.23	1.07	2.93	0.64	0	0.71	0.71	0.64	0
4.18	5.94	6.77	2.46	6.15	7.35	0.64	1.80	0.75	0.30	0.32	0
3.47	2.92	5.71	1.99	3.04	3.47	0.44	1.49	0.56	0.18	0.19	0
0.17	2.90	0.17	0.17	2.99	3.79	0.14	0.08	0.11	0.09	0.10	0
0	0.10	0	0	1.08	0.12	0	0	0	0	0	0
0	0	0	0	0	0	0.03	1.78	0.47	0.50	0.36	1.84
1.97	0.00	3.42	1.68	0	0	0.67	0.81	0.92	0.87	0.80	0.75
0	0	0	0	0	0	0	0	0	0	0	0
0	0	0	0	0	0	0	0	0	0	0	0
0.46	0.81	0.65	0.31	0.51	2.21	0.18	0.22	0.18	0.11	0.25	0.17
0.91	0.96	0.21	0.31	0.76	1.14	0.27	0.47	0.15	0.23	0.16	0.24
1.10	0.39	1.14	0.04	0.71	0	0	0.48	0	0	0	0.33
0	0	0	0	0	0	0	0	0	0	0	0
0	0	0	0	0	0	0	0	0	0	0	0
0	0	0	0	0	0	0	0	0	0	0	2.40
100	100	100	100	100	100	100	100	100	100	100	100
3	6	10	4	6	7	2	4	4	2	1	3
163	242	174	127	167	163	107	100	103	65	119	114
2295	1135	1685	805	2240	1588	455	210	249	64	125	439
5728	6317	5085	3498	6083	4974	1286	1500	1505	833	792	1468
3.0	4.5	4.2	1.6	4.4	3.9	0.93	1.6	1.0	1.1	0.5	0.9
48	46	58	43	59	80	10	16	10	19	14	12
22	26	34	16	41	34	13	12	15	14	12	16
4.1	5.6	6.9	3.0	6.6	6.5	0.93	1.6	0.9	1.3	0.7	1.1

TABLE 2 (continued)

	Cpx cumulate			Mafic syenite							
	6155	C6155	6169	751	816	832	915	6175	566	782	812
Ni	144	189	265	59	79	68	97	56	57	17	23
La	266.3	100.0	306.5	114.1	237.0	165.6	280.1	22.3	105.4	113.8	72.0
Ce	544.6	230.7	673.8	283.2	571.3	403.9	720.1	47.2	216.4	292.3	176.6
Nd	229.4	105.9	313.5	144.2	272.3	210.6	370.0	22.0	107.7	126.9	88.6
Sm	37.49	17.82	55.20	23.66	42.91	32.81	59.50	3.81	16.90	22.10	14.50
Eu	8.38	4.12	12.56	5.32	9.46	7.14	13.50	1.01	3.78	4.22	3.40
Tb	2.19	1.00	3.05	1.15	2.04	1.63	3.05	0.38	1.01	1.01	0.93
Yb	3.45	2.57	2.76	1.32	1.91	1.62	2.85	1.10	1.50	1.33	1.82
Lu	0.58	0.20	0.41	0.22	0.30	0.26	0.42	0.17	0.26	0.21	0.28
Zr	459	n.a.	337	232	259	226	375	125	184	119	256
Y	34	n.a.	50	26	34	30	44	13	24	27	29
Hf	11.7	10.0	7.8	4.5	5.0	3.9	7.4	2.9	4.2	2.4	4.7
Th	15.9	6.0	10.0	5.6	9.1	8.6	20.2	4.6	5.5	8.3	4.4
Nb	n.d.	n.d.	6	n.d.	2	1	8	3	n.d.	9	6
Ta	n.d.	0.11	0.7	0.2	0.6	0.1	1.0	0.4	0.3	0.75	0.5
(ppm)											

Fe_2O_3 as total iron; n.a.: not analysed; n.d.: not detected.

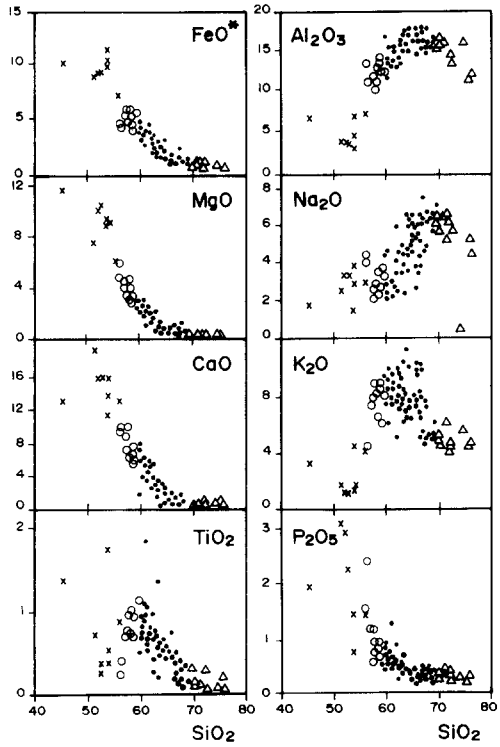

Fig. 5. Harker diagram showing the variation in major element abundances (wt.%) vs SiO_2 (wt.%) in the Clér-icy Pluton. Cross, clinopyroxene cumulate; open circle, mafic syenite; filled circle, felsic syenite; triangle, nord-markite; black star, calculated composition of the paren-tal magma.

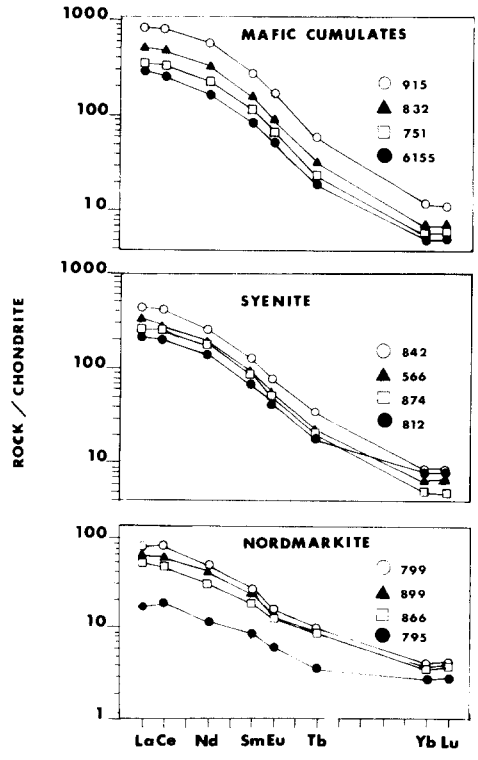

Fig. 6. Rare earth elements (REE) normalized to chon-drite. Chondrite normalizing values taken from Naka-mura (1974). See text for discussion.

Felsic syenite						Nordmarkite					
842	874	894	897	930	961	795	799	866	899	927	6178
12	20	22	10	23	17	10	10	10	9	8	9
139.7	83.6	113.0	32.5	126.5	510	5.4	23.4	16.2	17.7	16.4	13.6
354.3	218.3	226.8	77.5	287.1	1138	15.6	63.1	37.4	47.3	33.2	33.8
162.8	110.9	96.4	40.1	136.4	519	7.1	27.6	18.9	26.2	14.9	15.2
26.28	17.35	13.23	5.96	21.83	79.85	1.73	5.10	3.58	4.87	2.17	3.26
6.06	3.80	2.98	1.32	5.08	15.07	0.46	1.17	0.94	1.20	0.64	0.82
1.69	0.93	0.71	0.33	1.44	3.91	0.17	0.37	n.d.	0.42	0.24	0.31
1.90	1.11	1.20	0.60	1.42	2.71	0.60	0.85	0.78	0.68	0.48	0.69
0.29	0.17	0.21	0.10	0.22	0.37	0.10	0.14	0.12	0.10	0.07	0.1
209	228	135	83	197	171	122	135	128	47	23	142
35	22	22	15	27	48	11	14	14	11	12	14
4.0	5.3	2.6	1.7	3.6	4.3	3.4	3.5	3.8	4.6	0.7	4
25.2	7.9	8.1	4.1	9.6	39	3.0	6.7	10.4	1.7	1.4	10.4
11	11	n.d.	4	9	10	9	8	8	5	2	9
0.7	0.8	0.1	0.3	0.6	1.1	0.4	0.35	0.4	0.3	n.d.	0.5

the amphibole-bearing nordmarkites suggesting a relative loss of Rb.

Rare earth elements

Mafic syenites, felsic syenites and nordmarkites form, on the basis of their rare earth element (REE) patterns, three distinct groups representative of each intrusive facies (Fig. 6). The REE patterns of the felsic and mafic syenites are convex upward with a relative enrichment of the intermediate REE, a shape frequently encountered for clinopyroxenes of alkali basalts (Liotard et al., 1988). The La/Yb ratios decrease from 188 to 21 with increasing SiO_2 contents. Within the same interval, the chondrite-normalized values for La and Yb decrease from 1000 and 18 to 200 and 5, respectively. The decrease of La/Yb implies a bulk distribution coefficient $D_{La} \gg D_{Yb}$. This is in agreement with partition coefficients for sphene and apatite (Wörner et al., 1983; Lemarchand et al., 1987) which are present in the rocks. The nordmarkites have the lowest REE contents. Their REE patterns are different from those of the syenites but resemble some Archaean monzogranites closely associated with metasedimentary rocks in the central Pontiac Subprovince (e.g. Rive et al., 1990).

The negative Eu anomaly commonly found in some high SiO_2 peralkaline (e.g. Souther and Hickson, 1984) and differentiated shoshonitic (e.g. Pe-Piper, 1980) volcanic rocks is not present in the syenites and in the nordmarkites. This may be explained by high ratios of Eu^{3+}/Eu^{2+} in the syenitic and nordmarkitic melts (e.g. Mahood and Stimac, 1990) and/or by the strong decrease of the Eu partition coefficient with increasing melt peralkalinity (Drexler et al., 1983; Noble et al., 1979; Mahood and Stinac, 1990).

High field-strength elements (hfse)

As for REE, P_2O_5, Zr and Hf contents decrease from mafic to felsic syenites (Fig. 7, Table 2). Whereas the decrease of P_2O_5 can be related to apatite fractionation, the decrease of Zr and Hf cannot be accounted for by crystallization of zirconium-bearing phases (e.g. zircon, eudialyte) which are absent in the studied rocks. The combined effect of high peralkalinity, low lime and low f_{O_2} (absence of primary Fe–Ti oxides) in the syenitic melt strongly increase the zirconium solubility (e.g. Watson,

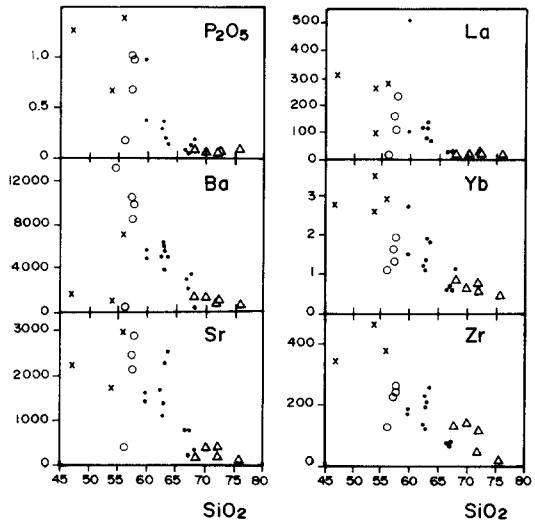

Fig. 7. Variation of trace element (ppm) and P_2O_5 (wt.%) against SiO_2 (wt.%) content in the Cléricy Pluton. Same symbols as in Fig. 5.

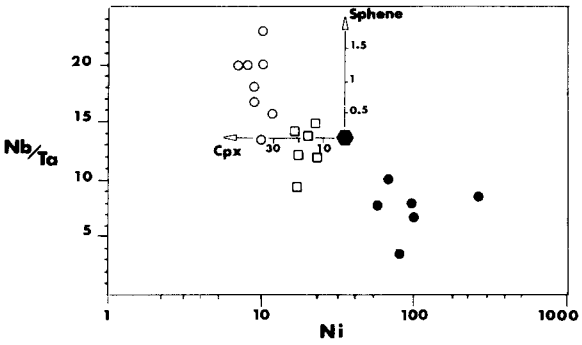

Fig. 8. Nb/Ta vs. Ni (ppm) showing the strong influence of sphene fractionation during magmatic differentiation. Fractionation vectors calculated using Rayleigh's law and distribution coefficients (K_d) from Wörner et al. (1983) and Wolff (1984). Filled circle, clinopyroxene cumulate; square, felsic syenite; open circle, nordmarkite; hexagon, parental magma calculated by numerical inversion.

1979; Jones and Peckett, 1980) and prevent zircon fractionation. This could explain the preferential partitioning of Zr (and Hf) in the Na-rich clinopyroxene. Furthermore, it is well known from detailed studies on peralkaline suites that Zr and Hf occur in considerable concentration (up to 2%) in Na-rich clinopyroxene (e.g. Larsen, 1976; Nielsen, 1979; Mahood and Stimac, 1990; Jones and Peckett,

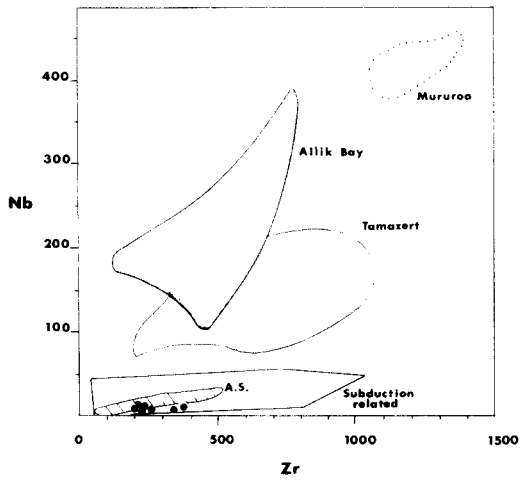

Fig. 9. Nb–Zr (ppm) plot modified from Thompson and Fowler (1986). Data for Tamazert from Bouabdli et al. (1988); Allik Bay from Malpas et al. (1986); Mururoa from Wagner et al. (1988). *A.S.* = Archaean shoshonite field from Brooks et al. (1982), Ujike (1985), Gentleman (1986) and Picard and Piboule (1986). Filled circle, most primitive syenite of the Cléricy Pluton.

1980). The fractionation of these Na-clinopyroxene will result in the lowering of the Zr and Hf abundances in the residual melts.

The average Zr/Hf ratio of mafic and felsic syenites is 50. This high value commonly encountered in Phanerozoic syenites, is also typical of highly undersaturated basalts. Nb and Ta contents are widely dispersed in the mafic and felsic syenites, but display no clear correlation with differentiation. However, the Nb/Ta ratios increase from 4 to 16 and are negatively correlated with Ni contents (Fig. 8). Because of the similarity of the bulk distribution coefficients for Nb and Ta in the major fractionating phases ($D_{Nb}=D_{Ta}$) (e.g. Wolff, 1984), the variation of the Nb/Ta ratio cannot reflect a dilution effect by feldspar and/or clinopyroxene accumulation. It rather reflects sphene fractionation or accumulation ($D_{Nb}^{sphene} < D_{Ta}^{sphene}$) as suggested by Wolff (1984).

The Nb/Zr ratios of the felsic syenites plot in the field of orogenic alkaline magmas (Fig. 9). Thus, the felsic syenites differ from intraplate syenites which are generally characterized by Nb/Zr ratio >100. The Ta/La

(<0.01) and Hf/Sm (<0.25) ratios are very low and are also characteristic of orogenic volcanic and associated plutonic rocks. The nordmarkites have the lowest high field-strength element (HFSE) contents and the average Zr/Hf ratio is 33. Such low HFSE contents (and Zr/Hf ratios) are different from those commonly observed in pre-kinematic plutonic rocks of the SAB (e.g. Paradis et al., 1988; Rive et al., 1990), but resemble values observed in Archaean metasedimentary and paragneissic rocks of the Pontiac Subprovince (e.g. Lajoie and Ludden, 1984; Ujike, 1984).

Transition elements

In the mafic and felsic syenites, transition element abundances are a function of the amount of clinopyroxene and correlate positively with CaO, MgO, and FeO, and negatively with Al_2O_3 and K_20 contents. When plotted against Ni on a log-scale diagram, some transition elements (e.g. Cr) display a linear variation suggesting that fractional crystallization has played some role during the differentiation (Fig. 10). The pronounced decrease of Co, Sc and V relative to Ni in the nordmarkites implies a change of bulk distribution coefficients. Indeed, an increase in the partition coefficients of these elements has been reported from highly polymerized magmas to which the nordmarkite magmas may be compared (Mahood, 1981; Wörner et al., 1983). However, an anomalously high Sc partition coefficient in clinopyroxene is needed to match Sc depletion in the nordmarkites (Fig. 10). This suggests that the nordmarkites cannot have been generated by fractional crystallization from a parental magma of felsic syenitic composition.

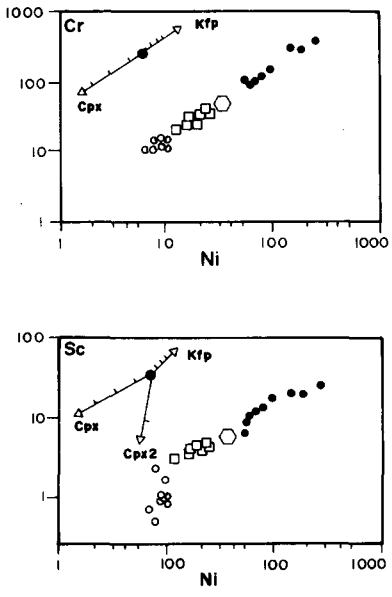

Fig. 10. Log Cr, Sc (ppm) vs. log Ni (ppm) diagram for the Clericy Pluton. Fractionation vectors calculated using Rayleigh's law and adequate K_d for K-feldspar and Cpx from Wörner et al. (1983), and Lemarchand et al. (1987). Same symbols as Fig. 8. Hexagon is parental magma calculated by numerical inversion. $K_{d(Ni,\,Cr,\,Sc)}^{Kfp/l}=0$ (Wörner et al., 1983); $K_{d(Ni,\,Cr,\,Sc)}^{Cpx/l}=5, 4.8, 4.2$ (Lemarchand et al., 1987); $K_{d(Sc)}^{Cpx2/l}=16$ ("Adjusted").

Isotopes

The isotopic data indicate a relatively large variation for the Rb–Sr and Sm–Nd isotopic systems (Table 3). The isotopic ratios correlate poorly with the corresponding parent–daughter ratios (Fig. 11). The slopes of the regression lines give an age of 2.07 ± 0.14 Ga for the Rb–Sr and 1.98 ± 0.27 Ga for Sm–Nd isotopic systems. These ages respectively become 2.13 ± 0.23 Ga and 3.41 ± 0.49 Ga when the nordmarkites are disregarded. The difference in the calculated ages may reflect contamination processes (e.g. Arndt and Jenner, 1986) and, to a lesser degree, the opening of the Sr isotopic system during the late pneumatolitic alteration event. Similar difficulties in age determination have been reported for the Abitibi Otto stock syenite (Bell and Blenkinsop, 1976) which is adjacent to the Timiskaming Group shoshonitic rocks. The true age of this intrusion, geologically similar to the Clériicy Pluton, has been recently defined, from precise U/Pb determination, at 2680 ± 1 Ma (Corfu et al., 1989) and is similar to the U/Pb ages obtained on other syenites (2.680 ± 4 Ma) from the eastern part of the Abitibi belt (Jamielita et al., 1990). Ages older than 3 Ga ob-

TABLE 3
Isotopic composition of Sr, Nd and Sm, Nd concentration for five samples and one clinopyroxene separated from cumulate

Sample	Name	Rb (ppm)	Sr (ppm)	$^{87}Sr/^{86}Sr$	Sm (ppm)	Nd (ppm)	$^{143}Nd/^{144}Nd$	$\epsilon_{Nd}(T)$
866	Nordmarkite	127	871	0.736516±24	3.41	17.21	0.511180±22	−1.9
6178	Nordmarkite	114	258	0.724288±28	2.86	14.77	0.511145±22	−1.7
566	Feld. syenite	177	1607	0.711355±20	19.21	126.8	0.510897±26	2.3
894	Feld.syenite	114	439	0.711579±22	13.55	98.59	0.510705±26	1.5
961	Feld. syenite	163	1577	0.711207±32	65.72	466.7	0.510694±28	0.6
618	Clinopyroxene	2	1615	0.701552±32	24.07	148.1	0.511010±32	2.2

$\epsilon_{Nd}(T)$ calculated at 2.68 Ga.
Age-corrected ratios have been calculated using bulk earth constants of $^{143}Nd/^{144}Nd = 0.512638$ and $^{147}Sm/^{144}Nd_{CHUR} = 0.1967$.

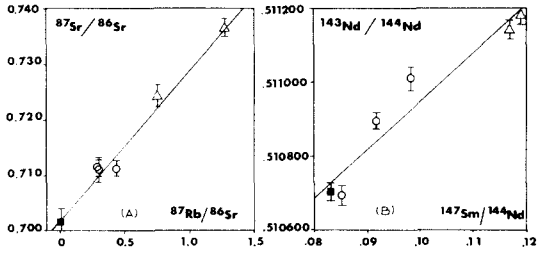

Fig. 11. A. $^{87}Rb/^{86}Sr$ vs. $^{87}Sr/^{86}Sr$ isochron diagram of the Clériçy Pluton. B. $^{147}Sm/^{143}Nd$ vs. $^{143}Nd/^{144}Nd$ isochron diagram of the Clériçy Pluton. The isochrons give ages of 2.07±0.14 Ga and 1.98±0.27 Ga for Rb–Sr and Sm–Nd isotopic systems. Initial isotopic ratios are $I_{Sr} = 0.701450$ and $I_{Nd} = 0.509645$. The regression lines are calculated according to the method of Minster et al. (1979). Error bars on $^{87}Sr/^{86}Sr$ and $^{143}Nd/^{144}Nd$ are from two sigma run statistics. Square, clinopyroxene; circle, felsic syenite; triangle, nordmarkite.

tained on the Clériçy Pluton are geologically unsound since they are older than the volcanic wall-rocks (Northern Blake River Group is 2698 Ma, Mortensen, 1987). In addition, no tectono-thermal event has been reported from this part of the Abitibi belt at 2 Ga. Detailed structural study has demonstrated that the Clériçy intrusion was affected by the end of the Archaean Kenoran Orogeny and also by late Archaean to early Proterozoic dextral strike-slip faulting. The latter event occurred between the end of the monzonitic to ultrapotassic magmatism in the southern Abitibi belt and the beginning of the Huronian sedimentation near 2.4 Ga.

It follows that the lines defined in Fig. 11 are more likely to be mixing lines involving a LREE-enriched component. This interpretation is further sustained by the progressive decrease of the ϵ_{Nd} initial ratio with increasing SiO_2 contents (Fig. 12B). This variation suggests contamination by a radiogenic crustal component similar in composition to some late Archaean metasedimentary rocks of the Abitibi belt (Dia et al., 1990). The DePaolo (1981) assimilation and fractional crystallization (AFC) equation was applied to the variation of the initial Nd isotopic ratio against Nd concentration in order to evaluate the effect of crustal contamination. The calculations reported in Fig. 12A indicate that the nordmarkitic compositions cannot be matched unless an unreasonably high proportion of crustal component is admitted. Thus, we suggest that the nordmarkites are representative of a liquid produced by partial melting of Archaean metasedimentary rocks or paragneiss slightly contaminated by syenitic liquid.

Even if it is assumed that the Rb/Sr isotopic ratios have been significantly modified by crustal contamination, it seems that some radiogenic loss of Rb or gain of ^{87}Sr occurred during late-stage pneumatolitic alteration. This is shown by the ϵ_{Sr} ratios ranging from −237 to −89 in the nordmarkites and −91 to −23 in the syenites (Table 3). For all six analysed samples, only the Rb–Sr isotopic system in the clinopyroxene remained closed during the pneumatolitic alteration. In the clinopyrox-

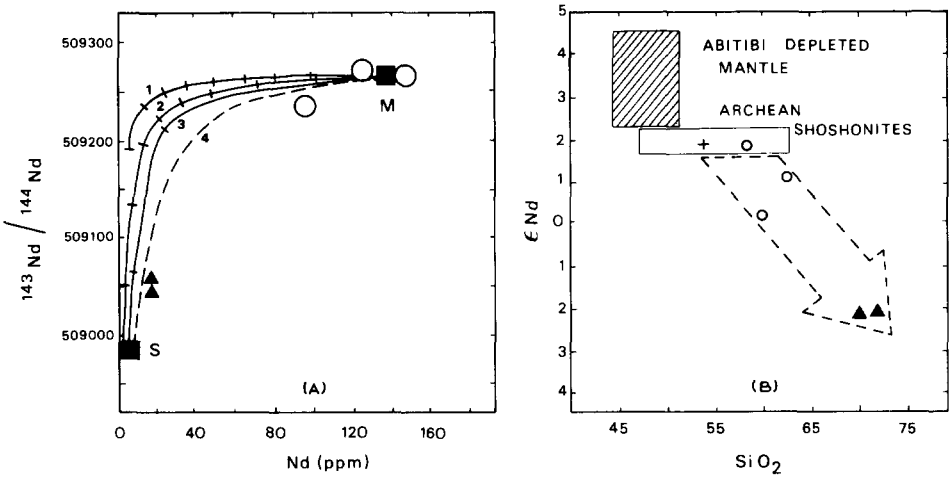

Fig. 12. A. Assimilation and fractional crystallization (AFC) (DePaolo, 1981) trends for crustal contamination of the Clériçy Pluton syenites. Numbers of the AFC trends refer to the model parameter R (assimilation rate); *1*: $R=0.2$; *2*: $R=0.5$; *3*: $R=0.9$; and *4*: to a simple mixing line. All AFC trends start at $F=0$ (relative amount of magma remaining) and are graduated in units of $F=0.10$ (ticks). D_{Nd} (bulk distribution coefficient) as been estimated graphically after the method of Allègre et al. (1977) and fixed at 2.0. *M*: initial syenitic magma; *S*: Archaean Abitibi metasedimentary rocks after Dia et al. (1990). Circle, felsic syenite; triangle, nordmarkite. B. ϵ_{Nd} (T) vs. SiO_2 (wt.%) for the Clériçy Pluton calculated at $T=2.68$ Ga. Abitibi depleted mantle from Dupré et al. (1985), and Smith and Ludden (1989). Archaean shoshonite field from Basu et al. (1984). (Same symbols as in Fig. 5.) See text for discussion.

ene, the $^{87}Sr/^{86}Sr$ measured ratio of 0.701552 ± 32 (Table 3) may closely approximate the initial $^{87}Sr/^{86}Sr$ ratio of the intrusion because of the very low Rb/Sr ratio. Even if time correction is not taken into account (age differences are less than 20 Ma), the clinopyroxene isotopic ratio is significantly higher when compared to the measured $^{87}Sr/^{86}Sr$ average ratio of 0.701131 ± 6 estimated for the Abitibi Archaean mantle (Machado et al., 1986). This may also be interpreted as further evidence for the influence of a crustal component.

On the basis of Hf isotope, Smith et al. (1987) also demonstrated the involvement of a radiogenic crustal component (different source reservoirs) during plutonism in the Michipicoten and Gamitagama greenstone belts of the Superior Province.

It is noteworthy that the two samples with the highest ϵ_{Nd} ratios (Fig. 12B) plot in the field of the Archaean Timiskaming Group shoshonitic rocks (Basu et al., 1984). This suggests a petrogenetic link between the syenites of the Clériçy Pluton and the Timiskaming volcanic Group (~2.7 Ga, Basu et al., 1984) which also contains sub-volcanic syenitic sills and stocks compositionally similar to the felsic syenites of the Clériçy Pluton (e.g. Kerrich and Watson, 1984).

Discussion

The chemical composition of the felsic syenites resembles those of differentiated alkaline magmas such as slightly aluminous trachytes (Wagner et al., 1988). On the other hand, the mafic syenites, characterized by high MgO contents and low FeO/MgO ratios, have no effusive equivalents in the alkaline rocks spectrum. Compared to shoshonites (Morrison, 1980; Meen, 1987) and phonolites (Wörner et al., 1983), the abundances of Al_2O_3 are too low and CaO too high. The cumulative nature of the mafic syenites is further indicated by Fig. 13. In this figure, the clinopyroxene cumulates and mafic syenites display relatively constant FeO/MgO, and high, but variable CaO/Al_2O_3

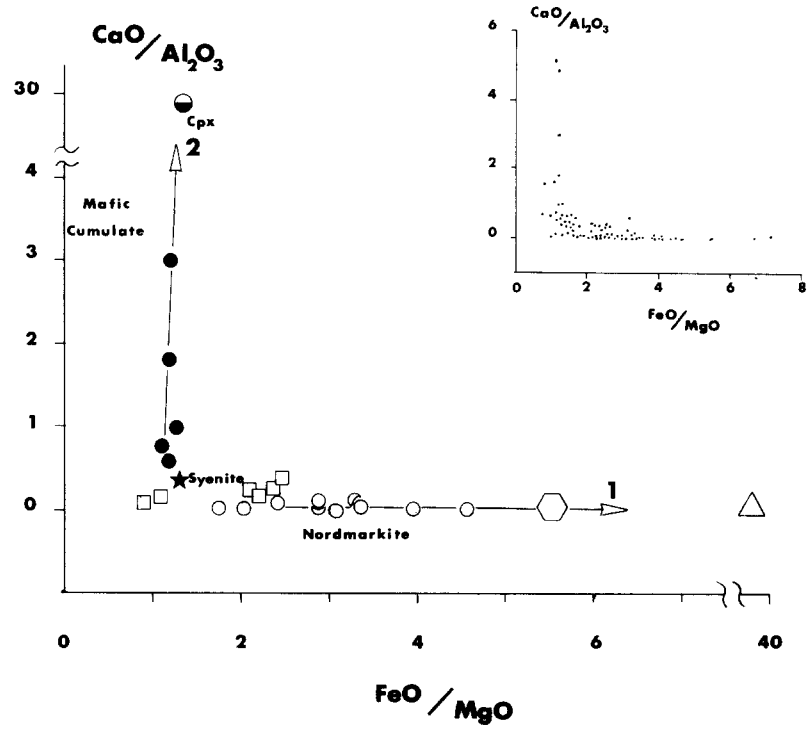

Fig. 13. CaO/Al_2O_3 vs. FeO/MgO plot. Vectors indicate magmatic fractionation (*1*) and crystal cumulation (*2*). Hexagon, comendite (from Bowden, 1974); triangle, comenditic obsidians (Nelson et al., 1987); black star, calculated parental magma.

ratios increasing proportionally with the clinopyroxene content. Enrichment of REE, HFSE and P_2O_5 in the mafic component suggests that sphene and apatite as well as clinopyroxene were cumulus phases.

The large range of composition found in the mafic syenites can be explained by a mixing line between two end-members with the compositions of primitive clinopyroxene and felsic syenitic liquid (trachytic magma) (Fig. 14). For example, sample 6155 (Table 2) approximately represents a mixture of 74% of the former and 26% of the latter. This suggests that some syenitic liquid was trapped within the cumulate component of the Clériсy intrusion. This feature, associated with field and textural observations, suggesting convection and disequilibrium growth of clinopyroxene in the more mafic rocks, is evidence of in-situ crystallization as described by Langmuir (1989). The correlated decreases of ϵ_{Nd} ratios and SiO_2 contents suggest an additional process of crustal contamination by an older silica-rich metasedimentary or gneissic component (Fig. 12B). Such crustal contamination is occasionally observed in more recent syenitic intrusions (e.g. Fowler, 1988). In the present case, this process is in agreement with the contrasting mineral chemistry typical of undersaturated alkaline rocks and the oversaturated character of the syenites shown by whole-rock analyses. Partial melting of the crustal component probably generated the late nordmarkitic dykes. When plotted on a quartz–albite–orthoclase diagram (Fig. 15), the particular major element composition of the nordmarkites can be interpreted as evidence of high P ($P_{H_2O} \geqslant 10$ kbar) (Yoder, 1968; Miller and Mittlefehldt, 1984) catazonal melt differentiation processes prior to melt extraction in the low-pressure plutonic environment. This hypothesis is further sustained by the trace element contents of

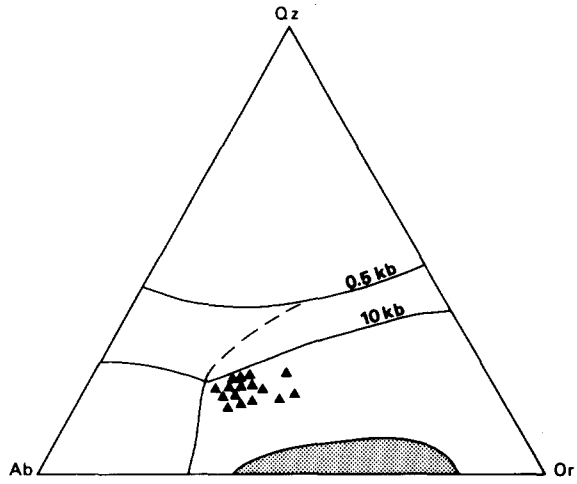

Fig. 14. V (ppm) vs. K_2O (wt.%) plot illustrating the mixing hypothesis between the clinopyroxene (Cpx) and the syenitic melt. See text for discussion.

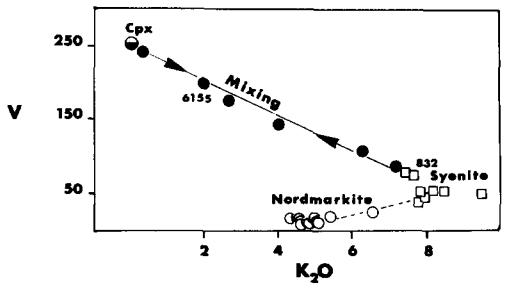

Fig. 15. Comparison of the range of composition between nordmarkitic dykes and syenites (symbol shape) of the Clériсy Pluton, in relation to the system Qz–Or–Ab–H_2O at 0.5 and 10 kbar.

these dykes which cannot be explained by in-situ fractional crystallization from a syenitic parental magma.

In the absence of samples coming from an outer chilled margin (covered by glacio-lacustrine sediments), we use a mass balance calculation based on the Tarantola and Valette (1982) algorithm of numerical inversion to evaluate the composition of the parental magma (Appendix A). In these mass balance equations we know the average concentration (C_{ij}) of an element (i) in a specific rock type (j), but other parameters used in the calculation (i.e. X_j and $C°$) are "a priori" values approximated independently.

The proportion (X_j) of each rock type has been evaluated directly from mapping (clinopyroxenitic enclave: $2 \pm 2\%$; mafic syenites: $40 \pm 15\%$; felsic syenites: $58 \pm 15\%$). The nordmarkites (10 to 15% of the pluton) are not taken into consideration since their chemistry is dominated by the presence of a crustal component.

The absence of orthopyroxene, olivine and Ca-plagioclase in the syenites and clinopyroxenitic enclaves as well as the low contents of Ni, do not support the presence of a parental magma in equilibrium with a mantle source. The similarity of initial Nd isotopic ratios in some samples of the Clériсy intrusion with those of the Timiskaming Group shoshonites (Basu et al., 1984) suggests that the parental magma ($C°$) had an evolved shoshonitic composition. Thus, the "a priori" $C°$ has been taken as the average chemical composition of Timiskaming Group shoshonites. This choice is favoured by the close geographical and time relationships between ultrapotassic plutonism (e.g. Clériсy Pluton) and shoshonitic volcanism (e.g. Timiskaming Group) in the southern Abitibi greenstone belt. It is also justified by the similarity of several trace element ratios such as Ta/La, Hf/Sm and Th/La of the Timiskaming Group shoshonites and the Clériсy syenites.

The calculated "a posteriori" values for the parental magma are in good agreement with petrological observations and are within the uncertainties related to the determinations of the "a priori" values (Table 4). The calculated "gain of information" is also consequential for both major (63%–88%) and trace element (36%–97%) data and justifies the validity of the calculation.

The calculated parental magma of the Clér-icy Pluton is characterized by strong REE fractionation, high Th content and strong HFSE depletion relative to REE. Geochemically it resembles modern shoshonitic rocks and related orogenic syenites (Fig. 16), but it differs from intraplate syenites which have distinctly higher Ta/La and Nb/Zr ratios (e.g. Fig. 9). The calculated parental magma can also be compared to shoshonites of the Roman comagmatic Province of Italy (e.g. Peccerillo et al., 1984; Peccerillo, 1985) and to some continental collision-related shoshonites (e.g. Thompson and Fowler, 1986). The available data on

TABLE 4
Calculated composition of the parental magma

C^{o*}	A-priori values		Adjusted values	
SiO_2	54	(10) [1]	620.4	(10.4)[2]
TiO_2	00.79	(0.45)	00.43	(0.14)
Al_2O_3	170.3	(70.1)	130.6	(10.2)
Fe_2O_3	8	(4)	40.2	(10.2)
MgO	3	(40.6)	20.4	(00.58)
CaO	60.0	(7)	40.9	(10.3)
Na_2O	30.8	(30.8)	40.2	(0.7)
K_2O	60.3	(60.9)	60.7	(10.0)
P_2O_5	00.56	(0.70)	00.51	(0.17)
Nb	110.2	(10)	6	(10.8)
Zr	280	(306)	180	(43)
Y	27	(20)	24	(5)
Sr	1340	(1077)	1459	(450)
Rb	176	(219)	131	(24)
La	105	(61)	100	(25)
Ce	206	(141)	230	(80)
Nd	85	(64)	107	(38)
Sm	160.6	(150.2)	180.7	(60.8)
Eu	40.02	(30.5)	40.2	(10.5)
Tb	10.30	(10.30)	10.10	(0.40)
Yb	20.43	(10.70)	10.37	(0.30)
Lu	00.34	(0.21)	00.21	(0.04)
Cu	54	(100)	21	(6)
Zn	103	(120)	59	(10)
Cr	37	(88)	61	(17)
Ba	3095	(4365)	4687	(1375)
Ni	18	(21)	35	(10)
Th	23	(22)	80.6	(30.7)
Ta	00.54	(0.37)	00.46	(0.15)
Hf	60.3	(60.5)	30.83	(00.9)
Sc	120.6	(21)	60.5	(10.6)
V	204	(183)	63	(13)
Co	20	(14)	9	(2)

A-priori values are from Ujike (1986) and Gentleman (1986). The values in brackets are the errors calculated by the inversion method (Tarantola and Valette, 1982), representing uncertainties in the parental magma composition before ([1]) and after ([2])inversion of the data. Standard variation for [1] and [2] is 3-σ level.

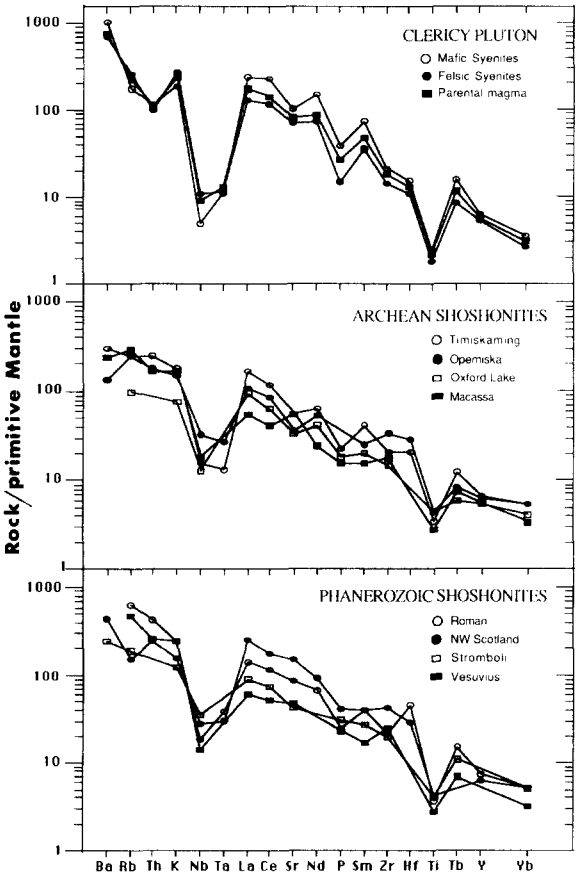

Fig. 16. Trace element concentrations of Archaean and Phanerozoic shoshonites (and related rocks) normalized to estimated primitive mantle composition (Sun and McDonough, 1989). Archaean shoshonitic rocks are from: Brooks et al. (1982); Ujike (1985); Gentleman (1986); Picard and Piboule (1986). Phanerozoic shoshonites: Dupuy et al. (1981); Peccerillo et al. (1984); Peccerillo (1985); Thompson and Fowler (1986).

Archaean shoshonitic volcanic and plutonic rocks of the Abitibi belt do not suggest any major chemical differences between Archaean and Phanerozoic shoshonites emplaced in non-oceanic (sialic) environments. However, some differences are obvious when the comparison is extended to typical oceanic-arc shoshonites (e.g. Gill and Whalen, 1989), which have lower K, Rb, Ba, Li and Th contents. This probably reflects the non-oceanic nature of the crust in the Abitibi belt during late-tectonic ultrapotassic magmatism.

Geotectonic and economic implications of Archaean ultrapotassic magmatism in the Abitibi greenstone belt

Although not identified in mid- to early Archaean cratons of Africa, Australia and Greenland, shoshonitic ultrapotassic magmatism is found in many late Archaean (2.7 Ga) greenstone belts of the Canadian Shield (Cooke and Moorhouse, 1969; Brooks et al., 1982; Picard and Piboule, 1986). This type of syn-orogenic or late-tectonic magmatism appears to be generally contemporaneous with the reactivation of major trans-lithospheric tectonic breaks (e.g. Larder Lake–Cadillac Break in the Abitibi greenstone belt in Fig. 1). In many cases, subaerial continental and/or fluvial types of sedimentation have been described (Hyde, 1978; Dimroth et al., 1981; Muëller and Dimroth, 1987) in the vicinity of these major faults suggesting rapid crustal growth and stabilization of the adjacent Archaean terranes. Major changes in the density and rheology of the Archaean lithosphere can be inferred from the palaeogeographic evolution from the early unstable subaqueous volcanic belts to the subsequent continental-type volcano-sedimentary activity. The stabilization of the Abitibi Archaean greenstone belt (following the Kenoran Orogeny) occurred more than 200 Ma before the beginning of the Proterozoic Era and required a rapid thickening of the Archaean lithosphere. Intensive intrusion of granodioritic magma at orogenic margins may be invoked as a possible mechanism of lithospheric thickening. Such a geotectonic environment is suggested in many cases by structural and geochemical observations which show clearly the syn- to late-orogenic nature of ultrapotassic volcanic and plutonic rocks (e.g. Oxford Lake Group, Manitoba, Brooks et al., 1982; Timiskaming Group, Ontario, Gentleman 1986; Opémisca Group, Québec, Picard and Piboule 1986).

Ultrapotassic and K-rich magmatism in the southern Abitibi belt which characterized the last 20 Ma of igneous activity (e.g. Jemielita et al., 1990) may be related to a subduction-driven accretion tectonic regime as suggested by Card (1990). This activity began with shoshonitic volcanism near major translithospheric faults (e.g. Cadillac Break) and culminated with K-rich plutonism which may represent an increasing rate of convergence and subduction of small heterogeneous plates.

Previous isotopic studies on komatiitic, basaltic (Dupré et al., 1984; Machado et al., 1986; Smith and Ludden, 1989), and differentiated volcanic rocks (Mortensen, 1987; Barrie and Shirey, 1989) of the southern Abitibi belt suggest that volcanic and plutonic rocks older than 2.7 Ga were derived from a depleted asthenospheric mantle with no ensialic "radiogenic" contribution. On the other hand, this study, and previous lead isotope analyses on some Abitibi late orogenic granitoids (Gariépy and Allègre, 1985) locally displaying S-type mineralogical characteristics, strongly suggest the presence of a "radiogenic" component underlying a part of the southern Abitibi greenstone belt.

The late appearance of a radiogenic crustal segment beneath the southern Abitibi belt is a possible explanation which is compatible with the subduction-driven accretion geotectonic framework proposed by Card (1990) for the Superior Province. At some time before the Archaean–Proterozoic transition, a part of the

southern Abitibi belt may have become allochthonous on the metasedimentary–plutonic Pontiac Subprovince. Structural analysis of the SAB–Pontiac transition (Goulet, 1978; Dimroth et al., 1983) near and to the south of the Larder Lake–Cadillac shear zone (Fig. 1), demonstrated the presence of overturn folds, stretching lineations and reverse faults dipping to the north. This, in agreement with the model proposed by Jackson and Sutcliffe (1990) and recent seismic-reflection profiles (Green et al., 1990; Jackson et al., 1990) suggesting the presence of subhorizontal faults or shear zones, may correspond to major deep thrusting under the southern limit of the greenstone belt.

The absence of significantly older gneisso-metasedimentary rocks in the vicinity of the SAB do not preclude this interpretation. It is obvious from recent geochronological studies in the Pontiac Subprovince (Mortensen et al., 1988) that the supracrustal and plutonic rocks are not significantly older than the Abitibi volcanic rocks. However, U–Pb systematics on single zircons (Gariépy et al., 1984) demonstrated the presence of several types of detrital zircons, some being approximately 2714 Ma, and others 2925–3000 Ma old. The significant contribution of 3000 Ma old sources in the metasedimentary rocks could easily explain the radiogenic enrichment observed in some late kinematic Abitibi granitoids and nordmarkites. Furthermore, metasedimentary or paragneissic rocks are suitable sources for peraluminous granitoids observed in the Val d'Or area of the SAB (e.g. Card et al., 1981).

In contrast with typical Archaean vertical tectonic models previously suggested for the southern Abitibi belt (e.g. "sagduction" and gravity tectonics, Goodwin and Smith, 1980; Jensen, 1985) and other Archaean supracrustal sequences (Vlaar, 1986), structural data (Goulet, 1978), seismic-reflection profiles (Green et al., 1990), palaeostratigraphic reconstitution (Dimroth et al., 1983; Thurston and Chivers, 1990), geochemical characteristics of the volcanic groups (e.g., Laflèche and Ludden, 1990) and the presence of Barovian-type metamorphism in the adjacent Pontiac Block (Jolly, 1980), suggest that a primitive form of plate subduction must have been operating in this part of the Superior Province during the late Archaean.

Compared to intraplate alkalic and carbonatitic complexes associated with continental rifts (e.g. Oslo, Norway, Andersen, 1984; St.-Laurent and Saguenay, Québec, Rondot, 1986) "orogenic" ultrapotassic suites such as those of the Abitibi belt and Scottish Caledonides (Thompson and Fowler, 1986) are generally devoid of "high technology metal deposits". Their absence in orogenic ultrapotassic suites can be interpreted as a consequence of the parental source having been depleted in Nb, Ta, Y, and HREE. As demonstrated in the present paper, the compatible behaviour of HFSE and REE during magmatic differentiation processes prevents their enrichment in highly differentiated components. On the other hand, gold mineralization and gold deposits are commonly associated with orogenic Archaean syenites. In the Abitibi greenstone belt, numerous structurally controlled gold deposits are related to syn-orogenic syenites (Kerrich and Watson, 1984; Yassa, 1987; Banfield, 1940) whereas late-tectonic syenites such as the Clériicy Pluton are devoid of gold mineralization.

Conclusions

The late tectonic Cléricy Pluton is one of the oldest known Archaean ultrapotassic syenitic intrusions. Its ultrapotassic and hypersolvus nature is characterized by a mineralogical assemblage dominated by perthitic potassic feldspar, Ca–Na clinopyroxene and minor amount of quartz.

Mafic to felsic syenites are the product of combined fractional crystallization of an evolved trachytic shoshonitic magma in a crustal environment under low P_{H_2O} (<2.5 kbar) and low f_{O_2} conditions, and magma mixing between the trachytic liquids and the

cumulative clinopyroxene-rich layers.

REE and HFSE (except Rb) behaved mainly as compatible elements suggesting sphene and apatite fractionation. The strong fractionation of the Nb/Ta ratio (4 to 16) also corroborates sphene fractionation and/or cumulation. On the other hand, the late peralkaline nordmarkitic dykes are the result of catazonal (high P^o) anatexis of metasedimentary rocks with some addition of syenitic magma.

It is noteworthy that the calculated parental magma of the Cléricy Pluton is an evolved (trachytic) shoshonite composition with chemical characteristics of Phanerozoic orogenic continental-type shoshonite.

Ultrapotassic magmatism in the SAB is related to a volcano-plutonic event characterizing the last 20 Ma of igneous activity in the Abitibi greenstone belt. It may represent an increased rate of convergence of small heterogeneous plates during a subduction-driven accretion tectonic event which possibly marked the culmination of the Kenoran Orogeny in the Superior Province of the Canadian Shield.

Acknowledgements

This study was conducted as part of the Ph.D. thesis requirements of the first author at the Université de Montpellier II (France) and conjointly with the C.N.R.S., Centre Géologique et Géophysique de Montpellier. In Canada, the research was supported and financed by Cambior Inc. Sincere appreciation is expressed to M. A.J. Ouellet, director of exploration and his team of field geologists in Rouyn-Noranda and Val d'Or, Québec. Isotopic analyses were kindly provided by F. and Ph. Vidal.

A first review of the manuscript was completed by G. Camiré of Carleton University (Ottawa). J.L. Bodinier and J. Vernières (C.N.R.S.) also provided valuable geochemical and mathematical insight into the "art" of modelling and numerical inversion. The authors would like to thank S.F. Foley, J.N. Ludden, B.G.J. Upton and an anonymous reviewer for their careful and critical reviews of the manuscript. M.R.L. also acknowledges financial support from F.C.A.R. (Québec).

Appendix A

The calculation of the major and/or trace element composition of the parental magma is based on the following mass-balance equations:

$$\vec{C}_n^0 = C_{n,m} \cdot \vec{X}_m \quad (1)$$

$$\vec{X}_m^T \cdot \vec{l}_m = 1 \quad (2)$$

where n represents the number of elements and m the number of facies in the intrusion. The vector $\vec{C}^0 \cong (C_i^0)$ stands for the chemical composition of the parental magma. $\mathbf{C} \cong (C_{ij})$ is the design matrix or data matrix, C_{ij} being the chemical composition of the element (i) in a facies (j) of the intrusion. The vector $\vec{X} \cong (X_j)$ represents ponderal percent of each facies of the pluton. $\vec{l}_m$ is the unity vector and T stands for the transpose.

In the present case, vectors $\vec{C}^0$ and $\vec{X}$ are the unknown, and the data matrix is only known within the limit of experimental and sampling uncertainty. Thus, we have to solve an undertermined system of $(n+1)$ relations and $(n+m)$ unknown. This problem is different from those usually investigated where the vector $\vec{C}^0$ is known, $\vec{X}$ being the unknown. Moreover, the n first relations (1) are only approximately known since the C_{ij} results from noisy data.

The calculation uses the algorithm of total inversion of Tarantola and Valette (1982). Following these authors, eqns. (1) and (2) may be changed as:

$$F(\vec{d}, \vec{p}) = 0 \quad (3)$$

where the vector $\vec{d}$; stands for the data $(C_{n,m})$ and the vector $\vec{p}$ for the unknown parameters ($\vec{C}^0$ and $\vec{X}$). F is the functional relation which

links $\vec{d}$ and $\vec{p}$ values through the model parameters, $\vec{C}^0$ and $\vec{X}$. Using a-priori values on $\vec{p}_0$ and $\vec{d}_0$ with their respectives uncertainties $\sigma(\vec{p}_0)$ and $\sigma(\vec{d}_0)$, we can obtain an estimation of the solution of the problem.

The algorithm is used to define the maximum likelihood solution $\vec{d}^*$, $\vec{p}^*$ and F as satisfying:

$$F(\vec{d}^*, \vec{p}^*) = 0 \tag{4}$$

This maximum likehood solution is defined as being the closest, in the least square sense, to the a-priori $\vec{d}_0$ and $\vec{p}_0$ values. p^* is computed iteratively using the fixed point algorithm of Tarantola and Valette (1982). The convergence is tested by that of the series:

$$\sum_{i=1}^{n+m} \frac{(p_i^k - p_i^{k+1})}{\mathrm{var}(p_i^{k+1})} \tag{5}$$

where k is the number of iteration and i the element in the vector $\vec{p}$.

The method allows estimation of an a-posteriori solution d^* and p^* associated with their respective a-posteriori error and control of the quality of the solution through the gain of information. This gain is expressed by the reduction of the a-posteriori error relative to the a-priori error.

Finally, the best fit of data is evaluated using the root means square:

$$\sqrt{\sum_{i=1}^{n+1} \frac{(d_i^* - d_{0,i})^2}{\mathrm{var}(d_i)}} \tag{7}$$

where $d_{0,i}$ and d_i are respectively elements of the $C_{n,m}$ and $C_{n,m}{}^*$ matrix.

References

Allègre, C.J., Treuil, M., Minster, J.F., Minster, B. and Albarède, F., 1977. Systematic use of trace element in igneous process. Part 1: fractional crystallization processes in volcanic suites. Contrib. Mineral. Petrol., 60: 57–75.

Allen, J.C. and Boettcher, A.L., 1978. Amphiboles in andesite and basalt, 1. Stability as a function of P–T–fO_2. Am. Mineral., 60: 1069–1085.

Ambrose, J.W., 1941. Regions de Cléricy et de la Pause, Québec. Commission géologique du Canada; Mémoir 233.

Andersen, T., 1984. Crystallization history of a Permian composite monzonite alkali syenite pluton in the Sande cauldron, Oslo rift, Southern Norway. Lithos, 17: 153–170.

Arndt, N.T and Jenner, G.A., 1986. Crustally contaminated komatiites and basalts from Kambalda, Western Australia. Chem. Geol., 56: 229–255.

Badham, J.P.N., 1979. Geology and petrochemistry of lower Aphebian (2.4–2.0 Ga) alkaline plutonic and hypabyssal rocks in the East Arm of Great Slave Lake, Northwest Territories. Can. J. Earth Sci., 16: 60–72.

Baker, P.E., 1975. Peralkaline acid volcanic rocks of Oceanic Islands. Bull. Volcanol., 38: 736–754.

Banfield, A.F., 1940. The Geology of Beattie Gold Mines (Quebec). Unpublished Ph.D. thesis, Western Ontario University, Ontario.

Bardintzeff, J.-M., Bellon, H., Bonin, B., Brousse, R. and McBirney, A.R., 1988. Plutonic rocks from Tahiti–Nui caldera (Society Archipelago, French Polynesia): a petrological, geochemical and mineralogical study. J. Volcanol. Geotherm. Res., 35: 31–53.

Barrie, C.T. and Shirey, S.B., 1989. Geochemistry and Nd–Sr isotope systematics of the Kamiskotia area, western Abitibi Subprovince, Canada: implications for mantle processes during the formation of the southern Superior Craton (Abstract). Lunar and planetary Institute, Houston, TX, Workshop on the Archean Mantle, Jan. 1989, 11–13.

Basu, A.R., Goodwin, A.M. and Tatsumoto, M., 1984. Sm–Nd study of Archean alkalic rocks from the Superior Province of the Canadian Shield. Earth Planet. Sci. Lett., 70: 40–46.

Bell, K. and Blenkinsop, J., 1976. A Rb–Sr whole-rock isochron from the Otto stock, Ontario. Can. J. Earth Sci., 13: 998–1002.

Bouabdli, A., Dupuy, C. and Dostal, J., 1988. Geochemistry of Mesozoic alkaline lamprophyres and related rocks from Tamazert massif, High Atlas Morocco. Lithos, 22: 43–58.

Brooks, C., Ludden, J.N., Pigeon, Y. and Hubregtse, J.J.M.W., 1982. Volcanism of shoshonite to high-K andesite affinity in an Archean arc environment, Oxford Lake, Manitoba. Can. J. Earth Sci., 19: 55–67.

Bowden, P., 1974. Oversaturated alkaline rocks: granites, pantellerites and comendites. In: H. Sorensen (Editor), The Alkaline Rocks. Wiley, New York, N.Y., pp. 109–123.

Card, K.D., 1990. A review of the Superior Province of the Canadian Shield, a product of Archean accretion. Precambrian Res., 48: 99–156.

Card, K.D., Percival, J.A., Lafleur, J. and Hogarth, D.D., 1981. Progress report on regional geological synthesis, central Superior Province. Geol. Surv. Can., 81-1a: 77–93.

Cooke, D.L. and Moorhouse, W.W., 1969. Timiskaming volcanism in the Kirkland Lake area, Ontario, Canada. Can. J. Earth Sci., 6: 117–132.

Corfu, F., Krogh, T.E., Kwok, Y.Y. and Jensen, L.S., 1989. U–Pb zircon geochronology in the southwestern Abitibi greenstone belt, Superior Province. Can. J. Earth Sci., 26: 1747–1763.

Currie, K.L., Eby, G.N. and Gittins, J., 1986. The petrology of the Mont St–Hilaire complex, southern Québec: an alkaline gabbro–peralkaline syenite association. Lithos, 19: 65–81.

Deer, W.A., Howie, R.A. and Zussman, J., 1978. Rock-Forming Minerals, Vol. 2A. Single-Chain Silicates. Longman, London, and Wiley, New York.

DePaolo, D.J., 1981. Trace element and isotopic effects of combined wallrock assimilation and fractional crystallization. Earth Planet. Sci. Lett., 53: 189–202.

Dia, A., Dupré, B., Gariépy, C. and Allègre, C.J., 1990. Sm–Nd and trace element characterization of shales from the Abitibi, Labrador Trough and Appalachian belts: consequences for crustal evolution through time. Can. J. Earth Sci. 27: 758–766.

Dimroth, E., Muller, W., Archer, P., Gobeil, A. and Allard, G.O., 1981. Evidence for extensive Archean shallow marine sedimentation in the Chibougamau area, Quebec. In: Current Research, Part A. Geol. Surv. Can., Pap., 82-1A: 29–36.

Dimroth, E., Imreh, L., Goulet, N. and Rocheleau, M., 1983. Evolution of the south-central segment of the Abitibi Belt, Québec, Part 3. Plutonic and metamorphic evolution and geotectonic model. Can. J. Earth Sci., 20: 1374–1388.

Dimroth, E., Imreh, L., Cousineau, P., Leduc, M. and Sanschagrin, Y., 1985. Paleogeographic analysis of mafic submarine flows and its use in the exploration for massive sulphide deposits. In: L.D. Ayres, P.C. Thurston, K.D. Card and Weber, W. (Editors), Evolution of Archean Supracrustal Sequences. Geol. Assoc. Can. Spec. Pap., 28: 203–222.

Dostal, J., Baragar, W.R.A. and Dupuy, C., 1986. Petrogenesis of the Natkusiak continental basalts, Victoria Island, N.W.T. Can. J. Earth Sci., 23: 622–632.

Drexler, J.W., Bornhorst, T.J. and Noble, D.C., 1983. Trace-element sanidine/glass distribution coefficients for peralkaline silicic rocks and their implications to peralkaline petrogenesis. Lithos, 16: 265–271.

Dupré, B., Chauvel, C. and Arndt, N.T.,1984. Pb and Nd isotopic study of two archean komatiitic flows from Alexo, Ontario, Geochim. Cosmochim. Acta, 48: 1965–1972.

Dupuy, C., Dostal, J., Girod, M. and Liotard, M., 1981. Origin of volcanic rocks from Stromboli (Italy). J. Volcanol. Geotherm. Res., 10: 49–65.

Ellam, R.M., Hawkesworth, C.J., Menzies, M.A. and Rogers, N.W., 1989. The volcanism of Southern Italy: role of subduction and the relationship between potassic and sodic alkaline magmatism. J. Geophys. Res., 94: 4589–4601.

Fahrig, W.F., 1985. The tectonic setting of continental mafic dyke swarms: failed arm and early passive margin. In: H.C. Halls and W.F. Fahrig (Editors), Mafic Dyke Swarms. Geol. Assoc. Can., Spec. Pap., 34: 331–348.

Foley, S.F., Venturelli, G., Green, D.H. and Toscani, L., 1987. The ultrapotassic rocks: characteristics, classification, and constraints for petrogenetic models. Earth Sci. Rev., 24: 81–134.

Fowler, M.B., 1988. Elemental evidence for crustal contamination of mantle-derived Caledonian syenite by metasediment anatexis and magma mixing. Chem. Geol., 69: 1–16.

Gariépy, C. and Allègre, C.J., 1985. The lead isotope geochemistry and geochronology of late-kinematic intrusives from the Abitibi greenstone belt, and the implications for late Archean crustal evolution. Geochim. Cosmochim. Acta, 49: 2371–2383.

Gariépy, C., Allègre, C.J. and Lajoie, J. 1984. U–Pb systematics in single zircons from the Pontiac sediments, Abitibi greenstone belt. Can. J. Earth Sci., 21: 1296–1304.

Gélinas, L., Brooks, C., Perrault, G., Carignan, J., Trudel, P. and Grasso, F., 1977. Chemo-Stratigraphic Divisions within the Abitibi Volcanic Belt, Rouyn–Noranda District, Quebec. In: W.R.A. Baragar, L.C. Coleman and J.M. Hall (Editors), Volcanic Regimes in Canada. Geol. Assoc. Can., Spec. Pap., 16: 265–295.

Gélinas, L., Trudel, P. and Hubert, C., 1984. Chemostratigraphic division of the Blake River Group, Rouyn–Noranda area, Abitibi, Quebec. Can. J. Earth. Sci., 21: 220–231.

Gentleman, S.M., 1986. Geochemistry and Petrogenesis of an Alkaline Suite, Kirkland Lake Abitibi Greenstone Belt, NE Ontario. Unpublished M.Sc. thesis, Université de Montréal, Québec.

Gill, J. and Whelan, P., 1989. Early rifting of an oceanic island arc (Fiji) produced shoshonitic to tholeiitic basalts. J. Geophys. Res., 94: 4561–4578.

Goodwin, A.M. and Ridler, R.H., 1970. The Abitibi orogenic belt. In: Symposium on Basins and Geosynclines of the Canadian Shield. Geol. Surv. Can. Pap., 70-40: 1–24.

Goodwin, A.M. and Smith, I.E.M., 1980. Chemical discontinuities in Archean metavolcanic terrains and the development of Archean crust. Precambrian Res., 10: 301–311.

Goulet, N., 1978. Stratigraphy and Structural Relationships Across the Cadillac–Larder Lake Fault, Rouyn–Beauchastel Area, Quebec. M.E.R.Q., DPV-602, 155 pp.

Green, A.G., Milkereit, B., Mayrand, L.J., Ludden, J.N., Hubert, C., Jackson, S.L., Sutcliffe, R.H., West, G.F., Verpaelst, P. and Simard, A., 1990. Deep structure of

an Archaean greenstone terrane. Nature, 344: 327–330.

Hyde, R.S., 1978. Sedimentology, Volcanology, Stratigraphy, and Tectonic Setting of the Archean Timiskaming Group, Abitibi Greenstone Belt, NE Ontario, Canada. Unpublished Ph.D. thesis, Mc Master University, Ontario.

Jackson, S.L. and Sutcliffe, R.H., 1990. Central Superior Province geology: evidence for an allochthonous, ensimatic, southern Abitibi greenstone belt. Can. J. Earth Sci., 27: 582–589.

Jackson, S.L., Sutcliffe, R.H., Ludden, J.N., Hubert, C., Mayrand, L.J., Green, A.G., Milkereit, B., West, G.F. and Verpaelst, P., 1990. Archean southern Abitibi greenstone belt: crustal srtucture from seismic reflection profiles. Geology. In press.

Jemielita, R.A., Davis, D.W. and Krogh, T.E., 1990. U–Pb evidence for Abitibi gold mineralization postdating greenstone magmatism and metamorphism. Nature, 346: 831–834.

Jensen, L.S., 1985. Stratigraphy and petrogenesis of Archean metavolcanic sequences, southwestern Abitibi Subprovince, Ontario. Geol. Assoc. Can., Spec. Pap., 28: 65–87.

Jolly, W.T., 1978. Metamorphic history of the Archean Abitibi belt. In: J.A. Fraser and W.W. Heywood (Editors), Metamorphism in the Canadian Shield. Geol. Surv. Ca., Pap., 78-10: 63–78.

Jolly, W.T., 1980. Development and degradation of Archean lavas, Abitibi Area, Canada, in light of major element geochemistry. J. Petrol., 21: 323–363.

Jones, A.P. and Peckett, A., 1980. Zirconium-bearing aegirines from Motzfeldt, South Greenland. Contrib. Mineral. Petrol., 75: 251–255.

Kerrich, R. and Watson, G.P., 1984. The Macassa mine Archean lode gold deposit, Kirkland Lake, Ontario: geology, patterns of alteration and hydrothermal regime. Econ. Geol., 79: 1104–1130.

Laflèche, M.R. and Ludden, J.N., 1991. The petrogenesis of Archean felsic magmas: implications from rhyolitic volcanics of the Superior Province of Canada. Submitted to: Precambrian Res.

Lajoie, J. and Ludden, J., 1984. Petrology of the Archean Pontiac and Kewagama sediments and implications for the stratigraphy of the southern Abitibi belt. Can. J. Earth. Sci., 21: 1305–1314.

Langmuir, C.H., 1989. Geochemical consequences of in situ crystallization. Nature, 340: 199–204.

Larsen, L.M., 1976. Clinopyroxenes and coexisting mafic minerals from the alkaline Ilimaussaq intrusion, South Greenland. J. Petrol., 17: 258–290.

Lemarchand, F., Villemant, B. and Calas, G., 1987. Trace elements distribution coefficients in alkali basalt series. Geochim. Cosmochim. Acta, 51: 1071–1082.

Liotard, J.-M., Briot, D. and Boivin, P., 1988. Petrological and geochemical relationships between pyroxene megacrysts and associated alkali-basalts from Massif Central (France). Contrib. Mineral. Petrol., 98: 81–90.

Luhr, J.F. and Carmichael, I.S.E., 1980. The Colina volcanic complex, Mexico. Contrib. Mineral. Petrol., 71: 343–372.

Machado, N., Brooks, C. and Hart, S.R., 1986. Determination of initial $^{87}Sr/^{86}Sr$ and $^{143}Nd/^{144}Nd$ in primary minerals from mafic and ultramafic rocks: experimental procedure and implications for the isotopic characteristics of the Archean mantle under the Abitibi greenstone belt, Canada. Geochim. Cosmochim. Acta, 50: 2335–2348.

Mahnes, G., Minster, J.F. and Allègre, C.J., 1978. Comparative U–Th–Pb and Rb–Sr study of St-Severin amphoterite: consequences for early solar system chronology. Earth Planet. Sci. Lett., 31: 14–24.

Mahood, G.A., 1981. Chemical evolution of a late Pleistocene rhyolite center: Sierra La Primavera, Jalisco, Mexico. Contrib. Mineral. Petrol., 77: 129–149.

Mahood, G.A. and Stimac, J.A., 1990. Trace-element partitioning in pantellerites and trachytes. Geochim. Cosmochim. Acta, 54: 2257–2276.

Malpas, J., Foley, S.F. and King, A.F., 1986. Alkaline mafic and ultramafic lamprophyres from the Aillik Bay area, Labrador. Can. J. Earth Sci., 23: 1902–1918.

Martin, R.F., 1969. The hydrothermal synthesis of low albite. Contrib. Mineral. Petrol., 23: 323–339.

Martin, R.F. and Bonin, B., 1976. Water and magma genesis: the association hypersolvus granite–subsolvus granite. Can. Mineral., 14: 228–237.

McBirney, A.R. and Aoki, K.I., 1968. Petrology of the island of Tahiti. Geol. Soc. Am., Mem., 116: 523–556.

Meen, K.M., 1987. Formation of shoshonites from calcalkaline basalt magmas: geochemical and experimental constraints from type locality. Contrib. Mineral. Petrol., 97, 333–351.

Miller, C.F. and Mittlefehldt, D.W., 1984. Extreme fractionation in felsic magma chambers: a product of liquid-stade diffusion or fractional crystallization? Earth Planet. Sci. Lett., 68: 151–158.

Minster, J.F., Ricard, L.P. and Allègre, C.J., 1979. ^{87}Rb–^{87}Sr chronology of enstatite meteorites. Earth Planet. Sci. Lett., 44: 420–440.

Morimoto, N., Fabries, J., Ferguson, A.K., Ginzburg, I.V., Ross, M., Seifert, F.A., Zussman, J., Aoki, K. and Gottardi, G., 1988. Nomenclature of pyroxenes. Am. Mineral., 73: 1123–1133.

Morrison, G.W., 1980. Characteristics and tectonic setting of the shoshonite rock association. Lithos, 13: 97–108.

Mortensen, J.K., 1987. Preliminary U–Pb zircon ages for volcanic and plutonic rocks of the Noranda–Lac Abitibi area, Abitibi Subprovince, Quebec. Geol. Surv. Can. Pap., 87-1a: 581–589.

Mortensen, J.K., Theriault, R.F. and Card, K.D., 1988. U–Pb and Rb–Sr age constraints for plutonism and

metamorphism in the Pontiac Subprovince and adjacent Grenville Province. In: Geol. Surv. Can. Pap., 88-1C: 93–99.

Muëller, W. and Dimroth, E. 1987. A terresterial–shallow marine transition in the Archean Opémisca Group, east of Chapais, Québec. Precambrian Res., 37: 29–55.

Nakamura, N., 1974. Determination of REE, Ba, Mg, Na and K in carbonaceous and ordinary chondrites. Geochim. Cosmochim. Acta, 38: 757–775.

Nelson, D.O., Nelson, K.L., Reeves, K.D. and Mattison, G.D., 1987. Geochemistry of Tertiary alkaline rocks of the Eastern Trans-Pecos magmatic Province, Texas. Contrib. Mineral. Petrol., 97: 40–45.

Nielsen, T.F.D., 1979. The occurence and formation of Ti-aegirines in peralkaline syenites. Contrib. Mineral. Petrol., 69: 235–244.

Noble, D.C., Rigot, W.L. and Bowman, H., 1979. Rare-earth element content of some highly differentiated ash-flow tuffs and lavas. Geol. Soc. Am. Spec. Pap., 180: 77–85.

OGS-MERQ, 1984. Lithostratigraphic Map of the Abitibi Subprovince. Ontario Geological Survey/Ministère de l'Energie et des Ressources, Québec Map 2484 in Ontario, D.V. 83-16 in Quebec.

Ojakangas, R.W., 1985. Review of Archean clastic sedimentation, Canadian Shield: major felsic volcanic contributions to turbidite and alluvial fan–fluvial facies associations. In: L.D. Ayres, P.C. Thurston, K.D. Card and W. Weber (Editors), Evolution of Archean Supracrustal Sequences. Geol. Assoc. Can. Spec. Pap., 8: 23–48.

Paradis, S., Ludden, J.N. and Gélinas, L.,; 1988. Evidence for contrasting compositional spectra in comagmatic intrusive and extrusive rocks of the late Archean Blake River Group, Abitibi, Quebec. Can. J. Earth Sci., 24: 1–25.

Peccerillo, A., 1985. Roman comagmatic Province (central Italy): Evidence for subduction-related magma genesis. Geology, 13: 103–106.

Peccerillo, A., Poli, G. and Tolomeo, L., 1984. Genesis, evolution and tectonic significance of K-rich volcanics from the Alban Hills (Roman comagmatic region) as infered from trace element geochemistry. Contrib. Mineral. Petrol., 86: 230–240.

Pe-Piper, G., 1980. Geochemistry of Miocene shoshonites, Lesbos, Greece. Contrib. Mineral. Petrol., 72: 387–396.

Percival, J.A., 1986. A possible exposed Conrad Discontinuity in the Kapuskasing uplift, Ontario. In: Reflection Seismology: The Continental Crust. Am. Geophys. Union, Washington, D.C., Geodyn. Ser., 14: 135–141.

Picard, C. and Piboule, M., 1986. Pétrologie des roches volcaniques du sillon de roches vertes archéennes de Matagami–Chibougamau à l'ouest de Chapais (Abitibi est, Québec), 2. Le groupe hautement potassique d'Opémisca. Can. J. Earth Sci., 23: 1169–1189.

Richard, P., Shimizu, N. and Allègre, C.J., 1976. $^{143}Nd/^{146}Nd$ a natural tracer: an application to oceanic basalts. Earth Planet. Sci. Lett., 31: 269–278.

Rive, M., 1989. Geological and Compilation Map of the Southern Abitibi Greenstone Belt, Rouyn–Noranda Area, Québec, Canada. Unpublished map, Min. En. Ress. Québec.

Rive, M., Pintson, H. and Ludden, J.N., 1990. Characteristics of late Archean plutonic rocks from the Abitibi and Pontiac subprovinces, Superior Province, Canada. In: M. Rive, P. Verpaelst, Y. Gagnon, J.M. Lulin, G. Riverin and A. Simard (Editors), The Northwestern Quebec Polymetallic Belt. The Canadian Institute of Mining and Metallurgy Material, Spec. Vol. 43.

Robert, F., 1989. Internal structure of the Cadillac tectonic zone southeast of Val d'Or, Abitibi belt, Quebec. Can. J. Earth Sci., 26; 2661–2690.

Rondot, J., 1986. Géosutures dans le Grenville. In: J.M. Moore, A. Davidson and A.J. Baer (Editors), The Grenville Province. Geol. Assoc. Can., Pap., 31.

Sakuyama, M., 1978. Evidence of magma mixing: petrological study of Shiroumaoike calc-alkaline andesite volcano, Japan. J. Volcanol. Geotherm. Res., 5: 179–208.

Santosh, M., Iyer, S.S., Vasconcellos, M.B.A. and Enzweiler, J., 1989. Late Precambrian alkaline plutons in southwest India: geochronologic and rare-earth element constraints on Pan-African magmatism. Lithos, 24: 65–79.

Smith, A.D. and Ludden, J.N., 1989. Nd isotopic evolution of the Precambrian mantle. Earth Planet. Sci. Lett., 93: 14–22.

Smith, P.E., Tatsumoto, M. and Fargubar, R.M., 1987. Zircon Lu–Hf systematics and the evolution of the Archean crust in the Superior Province, Canada. Contrib. Mineral. Petrol., 97: 93–104.

Sorensen, H. (Editor), 1974. The Alkaline Rocks. Wiley, London, 622 pp.

Souther, J.G. and Hickson, C.J., 1984. Crystal fractionation of the basalt comendite series of the Mount Edziza volcanic complex, British Columbia: major and trace elements. J. Volcanol. Geotherm. Res., 21: 79–106.

Streckeisen, A., 1976. To each plutonic rock its proper name. Earth Sci. Rev., 12: 1–33.

Sun, S.S. and McDonough, W.F., 1989. Chemical and isotopic systematics of oceanic basalts: Implications for mantle composition and processes. In: A.D. Saunders and M.J. Norry (Editors), Magmatism in the Ocean Basins. Geol. Soc. Spec. Publ., London, 42: 313–345.

Tarantola, A. and Valette, B. 1982. Inverse problems = quest for information. J. Geophys., 50: 159–170.

Thompson, R.N. and Fowler, M.B., 1986. Subduction-related shoshonitic and ultrapotassic magmatism: a study of Siluro–Ordovician syenites from Scottish Caledon-

ides. Contrib. Mineral. Petrol., 94: 507–522.

Thurston, P.C. and Chivers, K.M., 1990. Secular variation in greenstone sequence development emphasizing Superior Province, Canada. Precambrian Res., 46: 21–58.

Ujike, O., 1984. Chemical composition of Archean Ponti ac metasediments, southwestern Abitibi belt, Superior Province. Can. J. Earth Sci., 21: 727–730.

Ujike, O., 1985. Geochemistry of Archean alkalic volcanic rocks from the Crystal Lake area, east of Kirkland Lake, Ontario, Canada. Earth Planet. Sci. Lett., 73: 333–344.

Ujike, O. and Goodwin, A.M., 1987. Geochemistry and origin of Archean felsic metavolcanic rocks, central Noranda area, Quebec, Canada. Can. J. Earth Sci., 24: 2551–2567.

Upton, B.G.J. and Emeleus, C.H., 1987. Mid-Proterozoic alkaline magmatism in southern Greenland: the Gardar Province. In: J.G. Fitton and B.G.J. Upton (Editors), Alkaline Igneous Rocks. Geol. Soc. Spec. Publ., London, 30: 449–472.

Vlaar, N.J., 1986. Archean global dynamics. Geol. Mijnbouw, 65: 91–101.

Wagner, C., Guille, G., Coquillat, J.-L. and Velde, D., 1988. Zr-rich clinopyroxenes in a comenditic trachyte from Mururoa (French Polynesia). Bull. Mineral., 111: 523–534.

Wass, S.Y., 1979. Multiple origins of clinopyroxenes in alkali basaltic rocks. Lithos, 12: 115–132.

Watson, E.B., 1979. Zircon saturation in felsic liquids: experimental results and applications to trace element geochemistry. Contrib. Mineral. Petrol., 70: 407–419.

Wendlandt, R.F. and Eggler, D.H., 1980. The origins of potassic magmas, 1. Melting relations in the systems $KAlSiO_4$–Mg_2SiO_4–SiO_2 and $KAlSiO_4$–MgO–SiO_2–CO_2 to 30 kilobars. Earth Planet. Sci. Lett., 51: 215–220.

Wolff, J.A., 1984. Variation in Nb/Ta during differentiation of phonolitic magma, Tenerife, Canary Islands. Geochim. Cosmochim. Acta, 48: 1345–1348.

Wörner, G., Beusen, J.-M., Duchateau, N., Gijbels, R. and Schmincke, H.-U., 1983. Trace element abundances and mineral/melt distribution coefficients in phonolites from the Laacher See Volcano (Germany). Contrib. Mineral. Petrol., 84: 152–173.

Wyman, D.A and Kerrich, R., 1989. Archean lamprophyre dikes of the Superior Province, Canada: distribution, petrology, and geochemical characteristics. J. Geophys. Res., 94: 4667–4696.

Yassa, A., 1987. Rapport géologique de l'Indice d'Alembert (Central-Duparquet). Unpublished internal report, Cambior Inc. Rouyn–Noranda.

Yoder, H.S., 1968. Albite–anorthite–quartz–H_2O at 5 kb. Annu. Rep. Geophys. Lab., 66: 477–478.

Yoder, H.S., 1986. Potassium-rich rocks: phase analysis and heteromorphic relations. J. Petrol., 27: 1215–1228.